

Supporting Information for:

Exploiting spatial isomerism to modulate the assembled phases of compositionally identical sugar-based surfactants

Jia-Fei Poon,^a Alfonso Cabezón,^b Alessandro Gulotta,^c Najet Mahmoudi,^d Stefan Ulvenlund,^e Rebeca Garcia-Fandiño,^b Adrian Sanchez-Fernandez.^{f*}

^aEuropean Spallation Source, Box 176, SE-221 00 Lund, Sweden.

^bCenter for Research in Biological Chemistry and Molecular Materials (CIQUS), Department of Organic Chemistry, Universidade de Santiago de Compostela, Rúa de Jenaro de la Fuente, s/n, 15705 Santiago de Compostela, Spain.

^cDivision of Physical Chemistry, Department of Chemistry, Lund University, Box 124, SE-221 00 Lund, Sweden.

^dISIS Neutron and Muon Source, Science & Technology Facilities Council, Rutherford Appleton Laboratory, Chilton OX11 0QX, U.K.

^eDepartment of Process and Life Science Engineering, Lund University, Box 117, SE-221 00 Lund, Sweden.

^fCenter for Research in Biological Chemistry and Molecular Materials (CIQUS), Department of Chemical Engineering, University of Santiago de Compostela, Rúa de Jenaro de la Fuente, s/n, 15705 Santiago de Compostela, Spain.

*adriansanchez.fernandez@usc.es

Table of contents

1	Materials	2
2	Synthesis sugar-based surfactants	2
2.1	General	2
2.2	Synthetic procedure	2
2.3	NMR spectra	12
3	Methods	29
4	Data analysis	30
5	Supplementary results	31
5.1	Determination of the solubilisation temperature	32
5.2	Critical micelle concentration determination	32
5.3	DLS correlation curves	33
5.4	Results from SANS/SLS data analysis	33
5.5	MD simulation snapshots	34
5.6	Linear rheology results	34
5.7	Oscillatory rheology results	35
5.8	Cole-Cole plots	35
6	Supporting references	35

1 Materials

Reagents for surfactant synthesis were purchased from commercial suppliers and used without further purification. Aqueous solutions were prepared using deionised water of Mili-Q grade water (resistivity of 18.2 MΩ cm) or D₂O (Sigma-Aldrich, 99.9 atom %D).

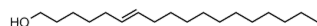
2 Synthesis sugar-based surfactants

2.1 General

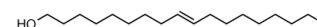
The precursors *cis*-vaccenic acid, *trans*-vaccenic acid,¹ (*Z*)-octadec-6-enoic acid,² (*E*)-octadec-6-enoic acid,³ and octadec-9-ynoic⁴ were synthesised according to literature procedures. Flash column chromatography was carried out using silica gel (40–63 μm, 230–400 mesh). ¹H and ¹³C NMR were recorded on a Bruker AVANCE spectrometer at 500 and 126 MHz, respectively, unless specified otherwise. High-resolution mass spectra were obtained on a Waters XEVO-G2 QTOF mass spectrometer. No melting point were determined as the sugar-based surfactants formed a glass upon heating.

2.2 Synthetic procedure

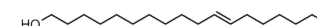
To LiAlH₄ (1.9 eq.) in anhydrous THF (30 mL) was dropwise added octadec-9-ynoic acid (1.0 eq.) in anhydrous THF (15 mL) under N₂ at 0 °C. After reflux for 3 hours, the reaction mixture was poured to ice-water followed by addition of sat. NH₄Cl solution (50 mL) and extraction with EtOAc (150 mL × 3). The organic phase was washed with brine (150 mL), dried over MgSO₄, filtered and evaporated under reduced pressure to afford the title compound.



(E)-Octadec-6-enol. To LiAlH₄ (760 mg, 20 mmol) in anhydrous THF (25 mL) was dropwise added (*E*)-octadec-6-enoic acid (3.0 g, 10.5 mmol) in anhydrous THF (13 mL) under N₂ at 0 °C. After reflux for 3 hours, the reaction mixture was poured to ice-water followed by addition of sat. NH₄Cl solution (50 mL) and extraction with EtOAc (150 mL × 3). The organic phase was washed with brine (150 mL), dried over MgSO₄, filtered and evaporated under reduced pressure to afford the title compound as pale yellow solid (2.8 g, 98%). ¹H NMR was in good agreement with reported data.⁵

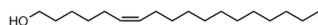


(E)-Octadec-9-enol. To LiAlH₄ (3.2 g, 84 mmol) in anhydrous THF (100 mL) was dropwise added (*E*)-octadec-9-enoic acid (12.6 g, 44.2 mmol) in anhydrous THF (50 mL) under N₂ at 0 °C. After reflux for 3 hours, the reaction mixture was poured to ice-water followed by addition of sat. NH₄Cl solution (50 mL) and extraction with EtOAc (150 mL × 3). The organic phase was washed with brine (150 mL), dried over MgSO₄, filtered and evaporated under reduced pressure to afford the title compound as white solid (12 g, quantitative). ¹H NMR was in good agreement with reported data.⁵

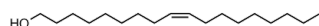


(E)-Octadec-11-enol. To LiAlH₄ (1.1 g, 30 mmol) in anhydrous THF (34 mL) was dropwise added (*E*)-octadec-11-enoic acid (4.3 g, 15.2 mmol) in anhydrous THF (15 mL) under N₂ at 0 °C. After reflux for 3 hours, the reaction mixture was poured to ice-water followed by addition

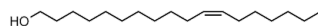
of sat. NH_4Cl solution (50 mL) and extraction with EtOAc (150 mL \times 3). The organic phase was washed with brine (150 mL), dried over MgSO_4 , filtered and evaporated under reduced pressure to afford the title compound as yellow oil (4.1 g, quantitative). ^1H NMR was in good agreement with reported data.⁶



(Z)-Octadec-6-enol. To LiAlH_4 (1.4 g, 37 mmol) in anhydrous THF (44 mL) was dropwise added (Z)-octadec-6-enoic acid (5.6 g, 19.8 mmol) in anhydrous THF (22 mL) under N_2 at 0 $^\circ\text{C}$. After reflux for 3 hours, the reaction mixture was poured to ice-water followed by addition of sat. NH_4Cl solution (50 mL) and extraction with EtOAc (150 mL \times 3). The organic phase was washed with brine (150 mL), dried over MgSO_4 , filtered and evaporated under reduced pressure to afford the title compound as pale yellow solid (5.3 g, quantitative). ^1H NMR was in good agreement with reported data.⁷



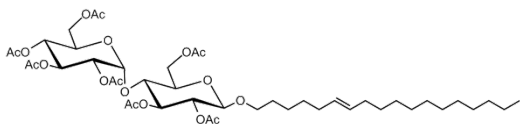
(Z)-Octadec-9-enol. To LiAlH_4 (1.6 g, 42 mmol) in anhydrous THF (50 mL) was dropwise added (Z)-octadec-9-enoic acid (6.3 g, 22.1 mmol) in anhydrous THF (25 mL) under N_2 at 0 $^\circ\text{C}$. After reflux for 3 hours, the reaction mixture was poured to ice-water followed by addition of sat. NH_4Cl solution (50 mL) and extraction with EtOAc (150 mL \times 3). The organic phase was washed with brine (150 mL), dried over MgSO_4 , filtered and evaporated under reduced pressure to afford the title compound as pale yellow oil (5.9 g, quantitative). ^1H NMR was in good agreement with reported data.⁸



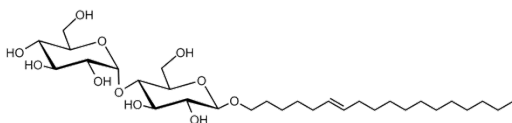
(Z)-Octadec-11-enol. To LiAlH_4 (1.4 g, 37 mmol) in anhydrous THF (44 mL) was dropwise added (Z)-octadec-9-enoic acid (5.5 g, 19.5 mmol) in anhydrous THF (22 mL) under N_2 at 0 $^\circ\text{C}$. After reflux for 3 hours, the reaction mixture was poured to ice-water followed by addition of sat. NH_4Cl solution (50 mL) and extraction with EtOAc (150 mL \times 3). The organic phase was washed with brine (150 mL), dried over MgSO_4 , filtered and evaporated under reduced pressure to afford the title compound as pale yellow solid (4.8 g, 92%). ^1H NMR was in good agreement with reported data.⁹



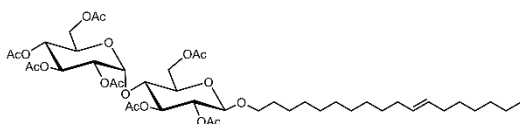
Octadec-9-yn-1-ol. To LiAlH_4 (905mg, 24 mmol) in anhydrous THF (30 mL) was dropwise added octadec-9-ynoic acid (3.5 g, 12.5 mmol) in anhydrous THF (15 mL) under N_2 at 0 $^\circ\text{C}$. After reflux for 3 hours, the reaction mixture was poured to ice-water followed by addition of sat. NH_4Cl solution (50 mL) and extraction with EtOAc (150 mL \times 3). The organic phase was washed with brine (150 mL), dried over MgSO_4 , filtered and evaporated under reduced pressure to afford the title compound as pale yellow solid (3.3 g, 99%). ^1H NMR was in good agreement with reported data.⁹



O-(E-6-octadecenyl) hepta-acetyl-maltose. To acetobromo- α -maltose (3.5 g, 5 mmol) in anhydrous DCM (27 mL) were added *E*-octadec-6-enol (2.7 g, 10 mmol) and 4Å molecular sieves (1.7 g) under N_2 at r.t. After stirring for 1 hour, Ag_2CO_3 (1.7 g, 6 mmol) and $AgClO_4$ (1.3 g, 6 mmol) were added. The reaction mixture was allowed to stir in dark for another 4 hours in prior to filtration through celite and evaporation under reduced pressure. The residue was purified by column chromatography using heptane/EtOAc (7:3) as eluent to afford the title compound as white solid (630 mg, 14%). 1H NMR (500 MHz, Chloroform-*d*) δ 5.41 (d, $J = 4.0$ Hz, 1H), 5.38 – 5.33 (m, 3H), 5.24 (t, $J = 9.0$ Hz, 1H), 5.04 (t, $J = 10.0$ Hz, 1H), 4.89 – 4.79 (m, 2H), 4.50 (d, $J = 8.0$ Hz, 1H), 4.46 (dd, $J = 12.0, 3.0$ Hz, 1H), 4.23 (ddd, $J = 12.5, 9.0, 4.0$ Hz, 2H), 4.05 – 3.94 (m, 3H), 3.83 (dt, $J = 9.5, 6.5$ Hz, 1H), 3.66 (ddd, $J = 10.0, 4.5, 2.5$ Hz, 1H), 3.45 (dt, $J = 10.0, 7.0$ Hz, 1H), 2.13 (s, 3H), 2.09 (s, 3H), 2.04 (s, 3H), 2.02 – 1.99 (m, 12H), 1.97 – 1.93 (m, 4H), 1.58 – 1.51 (m, 2H), 1.34 – 1.25 (s, 22H), 0.87 (t, $J = 7.0$ Hz, 3H). ^{13}C NMR (126 MHz, Chloroform-*d*) δ 170.51, 170.47, 170.3, 169.9, 169.6, 169.4, 130.7, 129.8, 100.3, 95.5, 75.5, 72.8, 72.2, 72.0, 70.2, 70.0, 69.3, 68.5, 68.0, 62.9, 61.5, 32.6, 32.5, 31.9, 29.7, 29.6, 29.5, 29.33, 29.28, 29.22, 29.18, 25.5, 25.3, 22.7, 20.9, 20.8, 20.7, 20.60, 20.59, 20.56, 20.55, 14.1. HRMS (ESI): Calc'd for $[Na+M]^+$: 909.4460, Found: 909.4460.

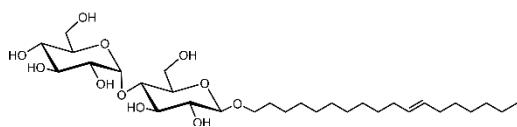


O-(E-6-octadecenyl)- β -D-maltopyranoside. To *O*-(*E*-6-octadecenyl) hepta-acetyl-maltose (560 mg, 0.6 mmol) in anhydrous MeOH (12 mL) was added dropwise a solution of NaOMe in MeOH (0.5 M, 1.8 mL, 0.9 mmol) at r.t. under N_2 . After stirring for 16 hours, the reaction mixture was neutralised with Amberlite 120 IR Hydrogen-form until pH = 5 – 6, prior to filtration and evaporation under reduced pressure. The residue was purified by column chromatography using heptane/EtOAc (7:3) \rightarrow DCM/MeOH (85:15) as eluent to afford the title compound as white powder (330 mg, 93%). 1H NMR (500 MHz, Methanol-*d*₄) δ 5.40 (m, 2H), 5.16 (d, $J = 3.5$ Hz, 1H), 4.26 (d, $J = 8.0$ Hz, 1H), 3.91 – 3.86 (m, 2H), 3.84 – 3.79 (m, 2H), 3.71 – 3.60 (m, 4H), 3.55 – 3.51 (m, 2H), 3.44 (dd, $J = 9.5, 4.0$ Hz, 1H), 3.38 – 3.34 (m, 1H), 3.28 – 3.21 (m, 2H), 2.05 – 1.96 (m, 4H), 1.62 (m, 2H), 1.40 – 1.29 (m, 22H), 0.90 (t, $J = 7.0$ Hz, 3H). ^{13}C NMR (126 MHz, Methanol-*d*₄) δ 131.6, 131.4, 104.32, 102.9, 81.3, 77.9, 76.6, 75.1, 74.8, 74.7, 74.2, 71.2, 70.9, 62.8, 62.2, 33.63, 33.60, 33.1, 30.77, 30.75, 30.7, 30.64, 30.59, 30.5, 30.2, 26.6, 23.7, 14.5. HRMS (ESI): Calc'd for $[Na+M]^+$: 615.3720, Found: 615.3727.

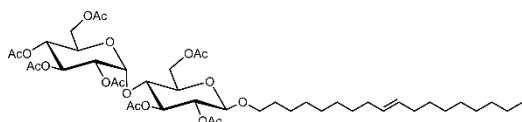


O-(E-11-octadecenyl) hepta-acetyl-maltose. To acetobromo- α -maltose (4.2g, 6 mmol) in anhydrous DCM (32 mL) were added *trans*-vaccenyl alcohol (3.2 g, 12 mmol) and 4Å molecular sieves (2.0 g) under N_2 at r.t. After stirring for 1 hour, Ag_2CO_3 (2.0 g, 7.2 mmol) and $AgClO_4$ (1.5 g, 7.2 mmol) were added. The reaction mixture was allowed to stir in dark for another 4 hours in prior to filtration through celite and evaporation under reduced pressure. The residue was purified by column chromatography using heptane/EtOAc (7:3) as eluent to

afford the title compound as white solid (850 mg, 16%). ¹H NMR (500 MHz, Chloroform-*d*) δ 5.40 (d, *J* = 4.0 Hz, 1H), 5.39 – 5.32 (m, 3H), 5.24 (t, *J* = 9.2 Hz, 1H), 5.04 (t, *J* = 9.9 Hz, 1H), 4.88 – 4.77 (m, 2H), 4.50 (d, *J* = 7.9 Hz, 1H), 4.46 (dd, *J* = 12.1, 2.8 Hz, 1H), 4.23 (ddd, *J* = 12.4, 8.7, 4.2 Hz, 2H), 4.07 – 3.92 (m, 3H), 3.83 (dt, *J* = 9.6, 6.4 Hz, 1H), 3.66 (ddd, *J* = 9.7, 4.4, 2.9 Hz, 1H), 3.45 (dt, *J* = 9.6, 6.8 Hz, 1H), 2.13 (s, 3H), 2.09 (s, 3H), 2.06 – 1.98 (m, 15H), 1.98 – 1.91 (m, 4H), 1.54 (h, *J* = 6.7, 6.2 Hz, 2H), 1.33 – 1.22 (m, 22H), 0.87 (t, *J* = 6.9 Hz, 3H). ¹³C NMR (126 MHz, Chloroform-*d*) δ 170.5, 170.5, 170.3, 169.9, 169.6, 169.4, 130.4, 130.3, 100.3, 95.5, 75.5, 72.8, 72.2, 72.0, 70.2, 70.0, 69.3, 68.4, 68.0, 62.9, 61.5, 32.6, 31.7, 29.62, 29.59, 29.57, 29.54, 29.48, 29.4, 29.3, 29.1, 28.8, 25.8, 22.6, 20.9, 20.8, 20.7, 20.59, 20.58, 20.54, 14.1. HRMS (ESI): Calc'd for [Na+M]⁺: 909.4460, Found: 909.4473.

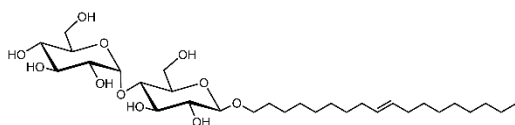


O-(E-11-octadecenyl)-β-D-maltopyranoside. To *O*-(*E*-11-octadecenyl) hepta-acetyl-maltose (780 mg, 0.9 mmol) in anhydrous MeOH (16 mL) was added dropwise a solution of NaOMe in MeOH (0.5 M, 2.5 mL, 1.3 mmol) at r.t. under N₂. After stirring for 16 hours, the reaction mixture was neutralised with Amberlite 120 IR Hydrogen-form until pH = 5 – 6, prior to filtration and evaporation under reduced pressure. The residue was purified by column chromatography using heptane/EtOAc (7:3) → DCM/MeOH (9:1) as eluent to afford the title compound as white powder (480 mg, 92%). ¹H NMR (500 MHz, Methanol-*d*₄) δ 5.39 – 5.37 (m, 2H), 5.16 (d, *J* = 3.8 Hz, 1H), 4.26 (d, *J* = 7.8 Hz, 1H), 3.93 – 3.85 (m, 2H), 3.85 – 3.77 (m, 2H), 3.72 – 3.57 (m, 4H), 3.57 – 3.49 (m, 2H), 3.44 (dd, *J* = 9.7, 3.8 Hz, 1H), 3.36 (ddd, *J* = 9.6, 4.6, 2.1 Hz, 1H), 3.29 – 3.19 (m, 2H), 1.98 (q, *J* = 6.2 Hz, 4H), 1.67 – 1.57 (m, 2H), 1.39 – 1.28 (m, 20H), 0.90 (t, *J* = 7.0 Hz, 3H). ¹³C NMR (126 MHz, Methanol-*d*₄) δ 131.5, 104.3, 102.9, 81.3, 77.9, 76.6, 75.1, 74.8, 74.7, 74.2, 71.5, 71.0, 62.8, 62.2, 33.6, 32.9, 30.81, 30.77, 30.7, 30.6, 30.6, 30.2, 29.9, 27.1, 23.7, 14.4. Calc'd for [Na+M]⁺: 615.3720, Found: 615.3720.

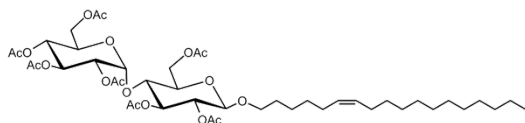


O-(E-9-octadecenyl) hepta-acetyl-maltose. To acetobromo-α-maltose (4.2g, 6 mmol) in anhydrous DCM (32 mL) were added trans-vaccenyl alcohol (3.2 g, 12 mmol) and 4Å molecular sieves (2.0 g) under N₂ at r.t. After stirring for 1 hour, Ag₂CO₃ (2.0 g, 7.2 mmol) and AgClO₄ (1.5 g, 7.2 mmol) were added. The reaction mixture was allowed to stir in dark for another 4 hours in prior to filtration through celite and evaporation under reduced pressure. The residue was purified by column chromatography using heptane/EtOAc (7:3) as eluent to afford the title compound as white solid (1.1 g, 20%). ¹H NMR (500 MHz, Chloroform-*d*) δ 5.40 (d, *J* = 4.0 Hz, 1H), 5.39 – 5.31 (m, 3H), 5.24 (t, *J* = 9.2 Hz, 1H), 5.04 (t, *J* = 9.8 Hz, 1H), 4.88 – 4.77 (m, 2H), 4.50 (d, *J* = 7.9 Hz, 1H), 4.46 (dd, *J* = 12.1, 2.8 Hz, 1H), 4.23 (ddd, *J* = 12.4, 8.8, 4.2 Hz, 2H), 4.06 – 3.92 (m, 3H), 3.83 (dt, *J* = 9.7, 6.4 Hz, 1H), 3.66 (ddd, *J* = 9.7, 4.4, 2.8 Hz, 1H), 3.45 (dt, *J* = 9.6, 6.8 Hz, 1H), 2.13 (s, 3H), 2.09 (s, 3H), 2.03 (s, 3H), 2.02 – 1.98 (m, 11H), 1.97 – 1.92 (m, 4H), 1.53 (p, *J* = 7.1, 6.6 Hz, 2H), 1.25 (s, 22H), 0.87 (t, *J* = 6.9 Hz, 3H). ¹³C NMR (126 MHz, Chloroform-*d*) δ 170.52, 170.47, 170.3, 169.9, 169.6, 169.4, 130.4, 130.2, 100.3, 95.5, 75.5, 72.8, 72.2, 72.0, 70.2, 70.0, 69.3, 68.4, 68.0, 62.9, 61.5, 32.57, 32.55, 31.9,

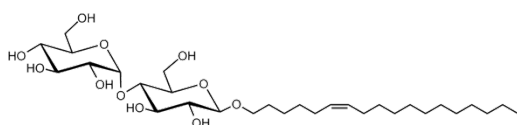
29.62, 29.61, 29.5, 29.44, 29.35, 29.28, 29.26, 29.2, 29.1, 25.8, 22.7, 20.9, 20.8, 20.7, 20.60, 20.58, 20.55, 14.1. Calc'd for [Na+M]⁺: 909.4460, Found: 909.4461.



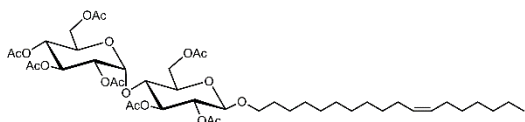
O-(E-9-octadecenyl)-β-D-maltopyranoside. To *O*-(*E*-9-octadecenyl) hepta-acetyl-maltose (920 mg, 1.0 mmol) in anhydrous MeOH (18 mL) was added dropwise a solution of NaOMe in MeOH (0.5 M, 2.9 mL, 1.5 mmol) at r.t. under N₂. After stirring for 16 hours, the reaction mixture was neutralised with Amberlite 120 IR Hydrogen-form until pH = 5 – 6, filtered and evaporated under reduced pressure. The residue was purified by column chromatography using heptane/EtOAc (7:3) → DCM/MeOH (9:1) as eluent to afford the title compound as white powder (600 mg, 97%). ¹H NMR (500 MHz, Methanol-*d*₄) δ 5.38 (td, *J* = 3.8, 1.9 Hz, 2H), 5.16 (d, *J* = 3.8 Hz, 1H), 4.26 (d, *J* = 7.8 Hz, 1H), 3.93 – 3.86 (m, 2H), 3.86 – 3.77 (m, 2H), 3.72 – 3.57 (m, 4H), 3.57 – 3.49 (m, 2H), 3.44 (dd, *J* = 9.7, 3.8 Hz, 1H), 3.36 (ddd, *J* = 9.6, 4.6, 2.1 Hz, 1H), 3.30 – 3.19 (m, 2H), 2.01 – 1.94 (m, 4H), 1.67 – 1.57 (m, 2H), 1.42 – 1.24 (m, 22H), 0.90 (t, *J* = 6.9 Hz, 3H). ¹³C NMR (126 MHz, Methanol-*d*₄) δ 131.5, 104.3, 102.9, 81.3, 77.9, 76.6, 75.1, 74.8, 74.7, 74.2, 71.5, 71.0, 62.8, 62.2, 33.62, 33.61, 33.0, 30.78, 30.76, 30.62, 30.59, 30.57, 30.5, 30.2, 27.1, 23.7, 14.5. Calc'd for [Na+M]⁺: 615.3720, Found: 615.3718.



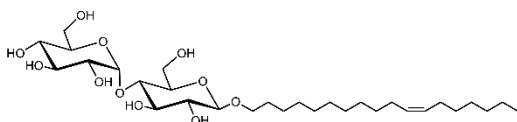
O-(Z-6-octadecenyl) hepta-acetyl-maltose. To acetobromo-α-maltose (4.2 g, 6 mmol) in anhydrous DCM (32 mL) were added *Z*-octadec-6-enol (3.2 g, 12 mmol) and 4Å molecular sieves (2 g) under N₂ at r.t. After stirring for 1 hour, Ag₂CO₃ (2 g, 7.2 mmol) and AgClO₄ (1.5 g, 7.2 mmol) were added. The reaction mixture was allowed to stir in dark for another 4 hours in prior to filtration through celite and evaporation under reduced pressure. The residue was purified by column chromatography using heptane/EtOAc (7:3) as eluent to afford the title compound as white solid (940 mg, 18%). ¹H NMR (500 MHz, Chloroform-*d*) δ 5.41 (d, *J* = 4.0 Hz, 1H), 5.37 – 5.30 (m, 3H), 5.24 (t, *J* = 9.5 Hz, 1H), 5.04 (t, *J* = 10.0 Hz, 1H), 4.87 – 4.79 (m, 2H), 4.50 (d, *J* = 8.0 Hz, 1H), 4.46 (dd, *J* = 12.0, 3.0 Hz, 1H), 4.24 (ddd, *J* = 12.0, 9.5, 4.0 Hz, 2H), 4.05 – 3.94 (m, 3H), 3.84 (dt, *J* = 9.5, 6.5 Hz, 1H), 3.68 – 3.65 (m, 1H), 3.46 (dt, *J* = 9.5, 7.0 Hz, 1H), 2.13 (s, 3H), 2.10 (s, 3H), 2.04 (s, 3H), 2.02 – 2.00 (m, 12H), 1.58 – 1.52 (m, 2H), 1.37 – 1.25 (s, 22H), 0.87 (t, *J* = 7.0 Hz, 3H). ¹³C NMR (126 MHz, CDCl₃) δ 170.52, 170.47, 170.3, 169.9, 169.6, 169.4, 130.2, 129.4, 100.3, 95.5, 75.5, 72.8, 72.2, 72.0, 70.1, 70.0, 69.3, 68.5, 68.0, 62.9, 61.5, 31.9, 29.7, 29.7, 29.62, 29.55, 29.4, 29.33, 29.31, 29.28, 27.2, 27.1, 25.5, 22.7, 20.9, 20.8, 20.7, 20.61, 20.59, 20.56, 20.55, 14.1. Calc'd for [Na+M]⁺: 909.4460, Found: 909.4468.



(Z-6-octadecenyl)- β -D-maltopyranoside. To *O*-(Z-6-octadecenyl)-hepta-acetyl-maltose (850 mg, 1.0 mmol) in anhydrous MeOH (17 mL) was added dropwise a solution of NaOMe in MeOH (0.5 M, 2.7 mL, 1.4 mmol) at r.t. under N₂. After stirring for 16 hours, the reaction mixture was neutralised with Amberlite 120 IR Hydrogen-form until pH = 5 – 6, filtered and evaporated under reduced pressure. The residue was purified by column chromatography using heptane/EtOAc (7:3) \rightarrow DCM/MeOH (9:1) as eluent to afford the title compound as white powder (560 mg, 98%). ¹H NMR (500 MHz, Methanol-*d*₄) δ 5.40 – 5.32 (m, 2H), 5.16 (d, *J* = 4.0 Hz, 1H), 4.27 (d, *J* = 8.0 Hz, 1H), 3.91 – 3.86 (m, 2H), 3.85 – 3.79 (m, 2H), 3.70 – 3.59 (m, 4H), 3.56 – 3.51 (m, 2H), 3.44 (dd, *J* = 9.5, 3.5 Hz, 1H), 3.36 (ddd, *J* = 9.5, 4.5, 2.0 Hz, 1H), 3.29 – 3.21 (m, 2H), 2.07 – 2.01 (m, 4H), 1.66 – 1.60 (m, 2H), 1.41 – 1.29 (m, 22H), 0.90 (t, *J* = 7.0 Hz, 3H). ¹³C NMR (126 MHz, Methanol-*d*₄) δ 130.9, 130.7, 104.3, 102.9, 81.3, 77.9, 76.6, 75.1, 74.8, 74.7, 74.2, 71.5, 70.9, 62.8, 62.2, 33.1, 30.84, 30.77, 30.75, 30.71, 30.6, 30.5, 30.3, 28.2, 28.1, 26.8, 23.7, 14.5. Calc'd for [Na+M]⁺ : 615.3720, Found: 615.3716.

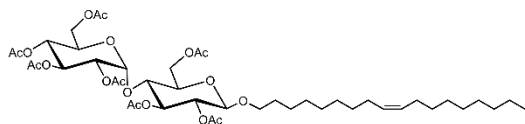


***O*-(Z-11-octadecenyl) hepta-acetyl-maltose.** To acetobromo- α -maltose (4.7g, 6.8 mmol) in anhydrous DCM (36 mL) were added *cis*-vaccenyl alcohol (3.6 g, 13.5 mmol) and 4Å molecular sieves (2.3 g) under N₂ at r.t. After stirring for 1 hour, Ag₂CO₃ (2.2 g, 8.1 mmol) and AgClO₄ (1.7 g, 8.1 mmol) were added. The reaction mixture was allowed to stir in dark for another 4 hours in prior to filtration through celite and evaporation under reduced pressure. The residue was purified by column chromatography using heptane/EtOAc (7:3) as eluent to afford the title compound as white solid (1.1 g, 19%). ¹H NMR (500 MHz, Chloroform-*d*) δ 5.41 (d, *J* = 4.0 Hz, 1H), 5.38 – 5.32 (m, 3H), 5.24 (t, *J* = 9.2 Hz, 1H), 5.04 (t, *J* = 9.9 Hz, 1H), 4.89 – 4.77 (m, 2H), 4.50 (d, *J* = 7.9 Hz, 1H), 4.46 (dd, *J* = 12.1, 2.8 Hz, 1H), 4.24 (ddd, *J* = 12.4, 8.7, 4.2 Hz, 2H), 4.07 – 3.92 (m, 3H), 3.83 (dt, *J* = 9.6, 6.4 Hz, 1H), 3.67 (ddd, *J* = 9.6, 4.4, 2.8 Hz, 1H), 3.46 (dt, *J* = 9.6, 6.8 Hz, 1H), 2.13 (s, 3H), 2.10 (s, 3H), 2.07 – 1.91 (m, 19H), 1.53 (p, *J* = 7.2, 6.7 Hz, 2H), 1.36 – 1.21 (m, 22H), 0.88 (m, *J* = 7.0 Hz, 3H). ¹³C NMR (126 MHz, Chloroform-*d*) δ 170.53, 170.48, 170.3, 170.0, 169.6, 169.4, 130.0, 129.8, 100.3, 95.5, 75.5, 72.8, 72.2, 72.0, 70.2, 70.0, 69.3, 68.5, 68.0, 62.9, 61.5, 31.8, 29.8, 29.7, 29.6, 29.6, 29.5, 29.4, 29.3, 29.3, 29.0, 27.2, 27.2, 25.8, 22.6, 20.9, 20.8, 20.7, 20.60, 20.59, 20.56, 20.55, 14.1. Calc'd for [Na+M]⁺ : 909.4460, Found: 909.4464.

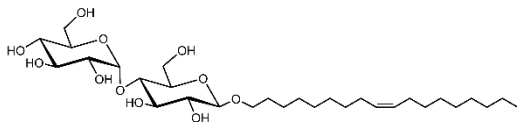


***O*-(Z-11-octadecenyl)- β -D-maltopyranoside.** To *O*-(Z-11-octadecenyl)-hepta-acetyl-maltose (750 mg, 0.85 mmol) in anhydrous MeOH (15 mL) was added dropwise a solution of NaOMe in MeOH (0.5 M, 2.4 mL, 1.2 mmol) at r.t. under N₂. After stirring for 16 hours, the reaction mixture was neutralised with Amberlite 120 IR Hydrogen-form until pH = 5 – 6, filtered and evaporated under reduced pressure. The residue was purified by column chromatography using heptane/EtOAc (7:3) \rightarrow DCM/MeOH (9:1) as eluent to afford the title compound as white powder (488 mg, 97%). ¹H NMR (500 MHz, Methanol-*d*₄) δ 5.41 – 5.30 (m, 2H), 5.16 (d, *J* = 3.8 Hz, 1H), 4.26 (d, *J* = 7.8 Hz, 1H), 3.93 – 3.85 (m, 2H), 3.85 – 3.77 (m, 2H), 3.72 – 3.57 (m,

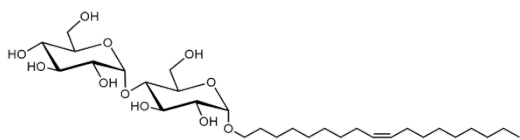
4H), 3.57 – 3.49 (m, 2H), 3.44 (dd, $J = 9.7, 3.8$ Hz, 1H), 3.39 – 3.32 (m, 1H), 3.31 – 3.19 (m, 3H), 2.07 – 1.94 (m, 4H), 1.67 – 1.57 (m, 2H), 1.44 – 1.22 (m, 22H), 0.91 (m, $J = 7.0$ Hz, 3H). ^{13}C NMR (126 MHz, Methanol- d_4) δ 130.8, 104.3, 102.9, 81.3, 77.9, 76.6, 75.1, 74.8, 74.7, 74.2, 71.5, 71.0, 62.8, 62.2, 32.9, 30.84, 30.83, 30.80, 30.75, 30.7, 30.6, 30.3, 30.0, 28.14, 28.12, 27.1, 23.7, 14.5. Calc'd for $[\text{Na}+\text{M}]^+$: 615.3720, Found: 615.3713.



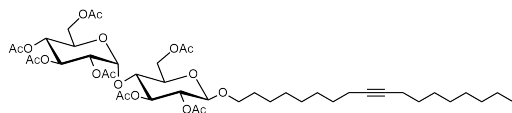
O-(Z-9-octadecenyl)-hepta-acetyl-maltose. To acetobromo- α -maltose (4.2g, 6 mmol) in anhydrous DCM (36 mL) were added oleyl alcohol (3.2 g, 12 mmol) and 4Å molecular sieves (2.0 g) under N_2 at r.t. After stirring for 1 hour, Ag_2CO_3 (2.0 g, 7.2 mmol) and AgClO_4 (1.5 g, 7.2 mmol) were added. The reaction mixture was allowed to stir in dark for another 4 hours in prior to filtration through celite and evaporation under reduced pressure. The residue was purified by column chromatography using heptane/EtOAc (7:3) as eluent to afford the title compound as white solid ($R_f = 0.18$, 1.1 g, 20%). ^1H NMR (500 MHz, Chloroform- d) δ 5.41 (d, $J = 4.0$ Hz, 1H), 5.38 – 5.30 (m, 3H), 5.24 (t, $J = 9.1$ Hz, 1H), 5.04 (t, $J = 9.9$ Hz, 1H), 4.89 – 4.77 (m, 2H), 4.50 (d, $J = 7.9$ Hz, 1H), 4.46 (dd, $J = 12.1, 2.8$ Hz, 1H), 4.24 (ddd, $J = 12.4, 8.7, 4.2$ Hz, 2H), 4.07 – 3.92 (m, 3H), 3.83 (dt, $J = 9.6, 6.4$ Hz, 1H), 3.70 – 3.62 (m, 1H), 3.46 (dt, $J = 9.6, 6.8$ Hz, 1H), 2.14 (s, 3H), 2.10 (s, 3H), 2.07 – 1.93 (m, 19H), 1.54 (dt, $J = 13.8, 6.8$ Hz, 2H), 1.35 – 1.24 (m, 22H), 0.87 (t, $J = 6.9$ Hz, 3H). ^{13}C NMR (126 MHz, Chloroform- d) δ 170.5, 170.3, 170.0, 169.6, 169.4, 130.0, 129.8, 100.3, 95.5, 75.5, 72.8, 72.2, 72.0, 70.2, 70.0, 69.4, 68.5, 68.0, 62.9, 61.5, 31.9, 29.7, 29.5, 29.4, 29.29, 29.28, 29.2, 27.19, 27.18, 25.8, 22.7, 20.9, 20.8, 20.7, 20.61, 20.59, 20.56, 14.1. Calc'd for $[\text{Na}+\text{M}]^+$: 909.4460, Found: 909.4464.



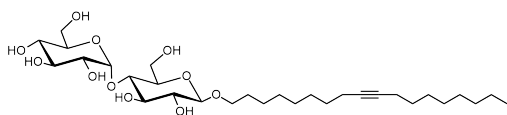
(Z-9-octadecenyl)- β -D-maltopyranoside. To *O*-(Z-9-octadecenyl)-hepta-acetyl-maltose (850 mg, 1.0 mmol) in anhydrous MeOH (17 mL) was added dropwise a solution of NaOMe in MeOH (0.5 M, 2.7 mL, 1.4 mmol) at r.t. under N_2 . After stirring for 16 hours, the reaction mixture was neutralised with Amberlite 120 IR Hydrogen-form until pH = 5 – 6, filtered and evaporated under reduced pressure. The residue was purified by column chromatography using heptane/EtOAc (7:3) \rightarrow DCM/MeOH (9:1) as eluent to afford the title compound as white powder (560 mg, 98%). ^1H NMR (500 MHz, Methanol- d_4) δ 5.34 (td, $J = 4.8, 4.0, 1.2$ Hz, 2H), 5.16 (d, $J = 3.8$ Hz, 1H), 4.26 (d, $J = 7.8$ Hz, 1H), 3.93 – 3.86 (m, 2H), 3.86 – 3.78 (m, 2H), 3.72 – 3.48 (m, 6H), 3.44 (dd, $J = 9.7, 3.8$ Hz, 1H), 3.36 (ddd, $J = 9.6, 4.6, 2.1$ Hz, 1H), 3.29 – 3.20 (m, 2H), 2.03 (q, $J = 6.4$ Hz, 4H), 1.67 – 1.57 (m, 2H), 1.41 – 1.25 (m, 22H), 0.90 (t, $J = 7.0$ Hz, 3H). ^{13}C NMR (126 MHz, Methanol- d_4) δ 130.8, 104.3, 102.9, 81.3, 77.9, 76.6, 75.1, 74.8, 74.7, 74.2, 71.5, 71.0, 62.8, 62.2, 33.1, 30.9, 30.83, 30.80, 30.64, 30.62, 30.60, 30.4, 30.34, 30.33, 28.2, 28.1, 27.1, 23.7, 14.5. Calc'd for $[\text{Na}+\text{M}]^+$: 615.3720, Found: 615.3727.



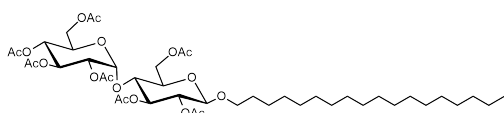
(Z-9-octadecenyl)- α -D-maltopyranoside. To acetobromo- α -maltose (4.2g, 6 mmol) in anhydrous DCM (36 mL) were added oleyl alcohol (3.2 g, 12 mmol) and 4Å molecular sieves (2.0 g) under N_2 at r.t. After stirring for 1 hour, Ag_2CO_3 (2.0 g, 7.2 mmol) and $AgClO_4$ (1.5 g, 7.2 mmol) were added. The reaction mixture was allowed to stir in dark for another 4 hours in prior to filtration through celite and evaporation under reduced pressure. The residue was purified by column chromatography using heptane/EtOAc (7:3 \rightarrow 5:5) as eluent. Fractions with $R_f = 0.09$ (heptane/EtOAc = 7:3) were collected and condensed under reduced pressure. The white waxy solid (700 mg) was re-dissolved in anhydrous MeOH (14 mL) in prior to addition of NaOMe in MeOH (0.5 M, 2.2 mL, 1.1 mmol) at r.t. under N_2 . After stirring for 24 hours, the reaction mixture was neutralised with Amberlite 120 IR Hydrogen-form until pH = 5 – 6, filtered and evaporated under reduced pressure. The residue was purified by column chromatography using heptane/EtOAc (7:3) \rightarrow DCM/MeOH (9:1) as eluent to afford the title compound as white powder (405 mg, 11% over 2 steps). 1H NMR (500 MHz, Methanol- d_4) δ 5.36 – 5.34 (m, 2H), 5.14 (d, $J = 3.5$ Hz, 1H), 4.76 (d, $J = 4.0$ Hz, 1H), 3.90 – 3.86 (m, 1H), 3.85 – 3.81 (m, 3H), 3.73 – 3.61 (m, 5H), 3.53 – 3.49 (m, 1H), 3.47– 3.42 (m, 3H), 3.27 (t, $J = 9.5$ Hz, 1H), 2.03 (q, $J = 6.0$ Hz, 4H), 1.67 – 1.59 (m, 2H), 1.41 – 1.29 (m, 22H), 0.90 (t, $J = 7.0$ Hz, 3H). ^{13}C NMR (126 MHz, Methanol- d_4) δ 130.8, 103.0, 100.0, 81.8, 75.1, 74.9, 74.8, 74.3, 73.2, 72.3, 71.5, 69.3, 62.7, 62.1, 33.1, 30.9, 30.84, 30.8, 30.64, 30.6, 30.45, 30.4, 30.3, 28.2, 28.1, 27.3, 23.7, 14.5. Calc'd for $[Na+M]^+$: 615.3720, Found: 615.3704.



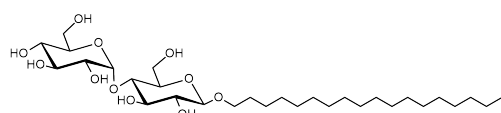
O-(9-octadecynyl)-hepta-acetyl-maltose. To acetobromo- α -maltose (4.1g, 5.8 mmol) in anhydrous DCM (32 mL) were added octadec-9-yn-1-ol (3.1 g, 11.6 mmol) and 4Å molecular sieves (2 g) under N_2 at r.t. After stirring for 1 hour, Ag_2CO_3 (2.2 g, 8.1 mmol) and $AgClO_4$ (1.7 g, 8.1 mmol) were added. The reaction mixture was allowed to stir in dark for another 3 hours in prior to filtration through celite and evaporation under reduced pressure. The residue was purified by column chromatography using heptane/EtOAc (7:3) as eluent to afford the title compound as white solid (840 mg, 16%). 1H NMR (500 MHz, Chloroform- d) δ 5.41 (d, $J = 4.0$ Hz, 1H), 5.35 (t, $J = 10.0$ Hz, 1H), 5.24 (t, $J = 9.5$ Hz, 1H), 5.04 (t, $J = 10.0$ Hz, 1H), 4.87 – 4.79 (m, 2H), 4.50 (d, $J = 8.0$ Hz, 1H), 4.46 (dd, $J = 12.0, 3.0$ Hz, 1H), 4.24 (ddd, $J = 12.0, 9.0, 4.0$ Hz, 2H), 4.05 – 3.94 (m, 3H), 3.83 (dt, $J = 10.0, 6.0$ Hz, 1H), 3.70 – 3.62 (m, 2H), 3.45 (dt, $J = 10.0, 6.5$ Hz, 1H), 2.14 – 2.10 (m, 10H), 2.04 – 2.00 (m, 15H), 1.58 – 1.52 (m, 2H), 1.49 – 1.43 (m, 4H), 1.38 – 1.25 (m, 18H), 0.87 (t, $J = 7.0$ Hz, 3H). ^{13}C NMR (126 MHz, $CDCl_3$) δ 170.52, 170.47, 170.3, 169.9, 169.6, 169.4, 100.3, 95.5, 80.3, 80.1, 75.5, 72.8, 72.2, 72.0, 70.2, 70.0, 69.3, 68.5, 68.0, 63.0, 62.9, 61.5, 32.8, 31.8, 29.4, 29.3, 29.20, 29.15, 29.13, 29.10, 28.9, 28.78, 28.76, 25.8, 25.7, 22.6, 20.9, 20.8, 20.7, 20.60, 20.59, 20.55, 18.7, 14.1. Calc'd for $[Na+M]^+$: 907.4307, Found: 907.4316.



(9-octadecynyl)- β -D-maltopyranoside. To *O*-(9-octadecynyl)-hepta-acetyl-maltose (730 mg, 0.8 mmol) in anhydrous MeOH (15 mL) was added dropwise a solution of NaOMe in MeOH (0.5 M, 2.3 mL, 1.2 mmol) at r.t. under N_2 . After stirring for 16 hours, the reaction mixture was neutralised with Amberlite 120 IR Hydrogen-form until pH = 5 – 6, filtered and evaporated under reduced pressure. The residue was purified by column chromatography using heptane/EtOAc (7:3) \rightarrow DCM/MeOH (85:15) as eluent to afford the title compound as white powder (450 mg, 95%). 1H NMR (500 MHz, Methanol- d_4) δ 5.16 (d, J = 4.0 Hz, 1H), 4.27 (d, J = 8.0 Hz, 1H), 3.91 – 3.87 (m, 2H), 3.84 – 3.79 (m, 2H), 3.70 – 3.59 (m, 4H), 3.56 – 3.51 (m, 2H), 3.44 (dd, J = 10.0, 4.0 Hz, 1H), 3.36 (ddd, J = 10.0, 4.5, 2.5 Hz, 1H), 3.28 – 3.20 (m, 2H), 2.13 – 2.10 (m, 4H), 1.65 – 1.60 (m, 2H), 1.49 – 1.29 (m, 22H), 0.91 (t, J = 7.0 Hz, 3H). ^{13}C NMR (126 MHz, MeOD) δ 104.3, 102.9, 81.3, 80.9, 77.9, 76.6, 75.1, 74.8, 74.7, 74.2, 71.5, 70.9, 62.8, 62.2, 33.0, 30.8, 30.7, 30.4, 30.28, 30.25, 30.24, 30.22, 29.9, 29.8, 27.1, 23.7, 19.4, 14.5. Calc'd for $[Na+M]^+$: 613.3564, Found: 613.3563.



***O*-(octadecyl)-hepta-acetyl-maltose.** To acetobromo- α -maltose (4.2g, 6.0 mmol) in anhydrous DCM (32 mL) were added stearyl alcohol (3.3 g, 12 mmol) and 4Å molecular sieves (2 g) under N_2 at r.t. After stirring for 1 hour, Ag_2CO_3 (2.0 g, 7.2 mmol) and $AgClO_4$ (1.5 g, 7.2 mmol) were added. The reaction mixture was allowed to stir in dark for another 3 hours in prior to filtration through celite and evaporation under reduced pressure. The residue was purified by column chromatography using heptane/EtOAc (7:3) as eluent to afford the title compound as white solid (840 mg, 16%). 1H NMR (500 MHz, Chloroform- d) δ 5.41 (d, J = 4.0 Hz, 1H), 5.35 (dd, J = 10.5, 9.5 Hz, 1H), 5.24 (t, J = 9.0 Hz, 1H), 5.04 (t, J = 10.0 Hz, 1H), 4.87 – 4.79 (m, 2H), 4.50 (d, J = 8.0 Hz, 1H), 4.46 (dd, J = 12.0, 3.0 Hz, 1H), 4.24 (ddd, J = 12.5, 9.0, 4.5 Hz, 2H), 4.05 – 3.94 (m, 3H), 3.83 (dt, J = 9.5, 6.5 Hz, 1H), 3.66 (ddd, J = 9.5, 4.0, 2.5 Hz, 1H), 3.46 (dt, J = 10.0, 6.5 Hz, 1H), 2.13 (s, 3H), 2.10 (s, 3H), 2.04 – 2.00 (m, 15H), 1.56 – 1.52 (m, J = 2H), 1.30 – 1.24 (m, 30H), 0.87 (t, J = 6.9 Hz, 3H). ^{13}C NMR (126 MHz, $CDCl_3$) δ 170.52, 170.47, 170.3, 169.9, 169.6, 169.4, 100.3, 95.5, 75.45, 72.8, 72.2, 72.0, 70.2, 70.0, 69.3, 68.5, 68.0, 62.9, 61.5, 31.9, 29.67, 29.66, 29.63, 29.60, 29.4, 29.3, 29.3, 25.8, 22.7, 20.9, 20.8, 20.7, 20.61, 20.59, 20.56, 20.55, 14.1.



***O*-octadecyl- β -D-maltopyranoside.** To *O*-(octadecanyl)-hepta-acetyl-maltose (740 mg, 0.8 mmol) in anhydrous MeOH (45 mL) was added dropwise a solution of NaOMe in MeOH (0.5 M, 2.3 mL, 1.2 mmol) at r.t. under N_2 . After stirring for 16 hours, the reaction mixture was neutralised with Amberlite 120 IR Hydrogen-form until pH = 5 – 6, filtered and evaporated under reduced pressure. The residue was purified by column chromatography using heptane/EtOAc (7:3) \rightarrow DCM/MeOH (9:1) as eluent to afford the title compound as white

powder (450 mg, 91%). ^1H NMR (500 MHz, Methanol- d_4) δ 5.16 (d, $J = 4.0$ Hz, 1H), 4.26 (d, $J = 7.5$ Hz, 1H), 3.91 – 3.87 (m, 2H), 3.84 – 3.79 (m, 2H), 3.70 – 3.60 (m, 5H), 3.56 – 3.51 (m, 2H), 3.44 (dd, $J = 9.5, 4.0$ Hz, 1H), 3.36 (ddd, $J = 9.5, 4.5, 2.0$ Hz, 1H), 3.28 – 3.20 (m, 2H), 1.65 – 1.59 (m, 2H), 1.41 – 1.29 (s, 30H), 0.90 (t, $J = 7.0$ Hz, 3H). ^{13}C NMR (126 MHz, MeOD) δ 104.3, 102.9, 81.4, 77.9, 76.6, 75.1, 74.8, 74.7, 74.2, 71.5, 71.0, 62.8, 62.2, 33.1, 30.78, 30.76, 30.6, 30.5, 27.1, 23.7, 14.4.

2.3 NMR spectra

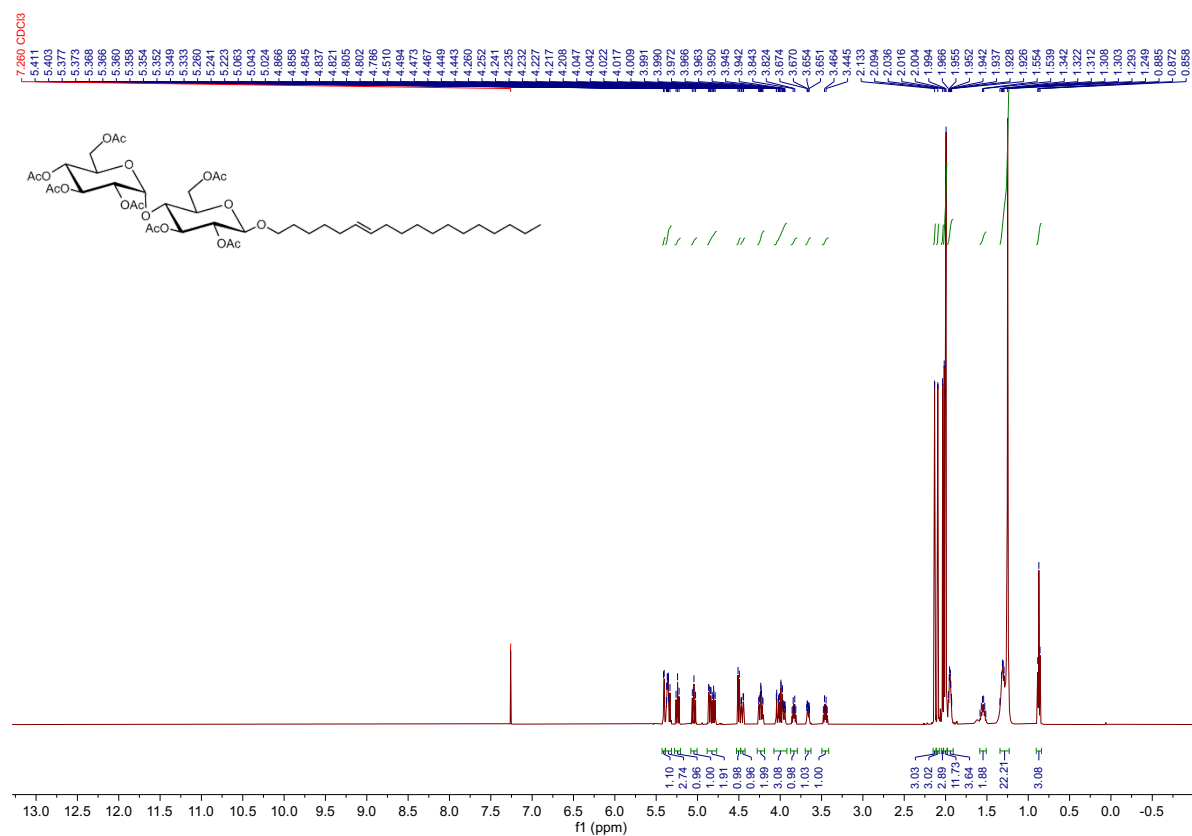


Fig. S1. ^1H NMR spectrum of *O*-(*E*-6-octadecenyl) hepta-acetyl-maltose.

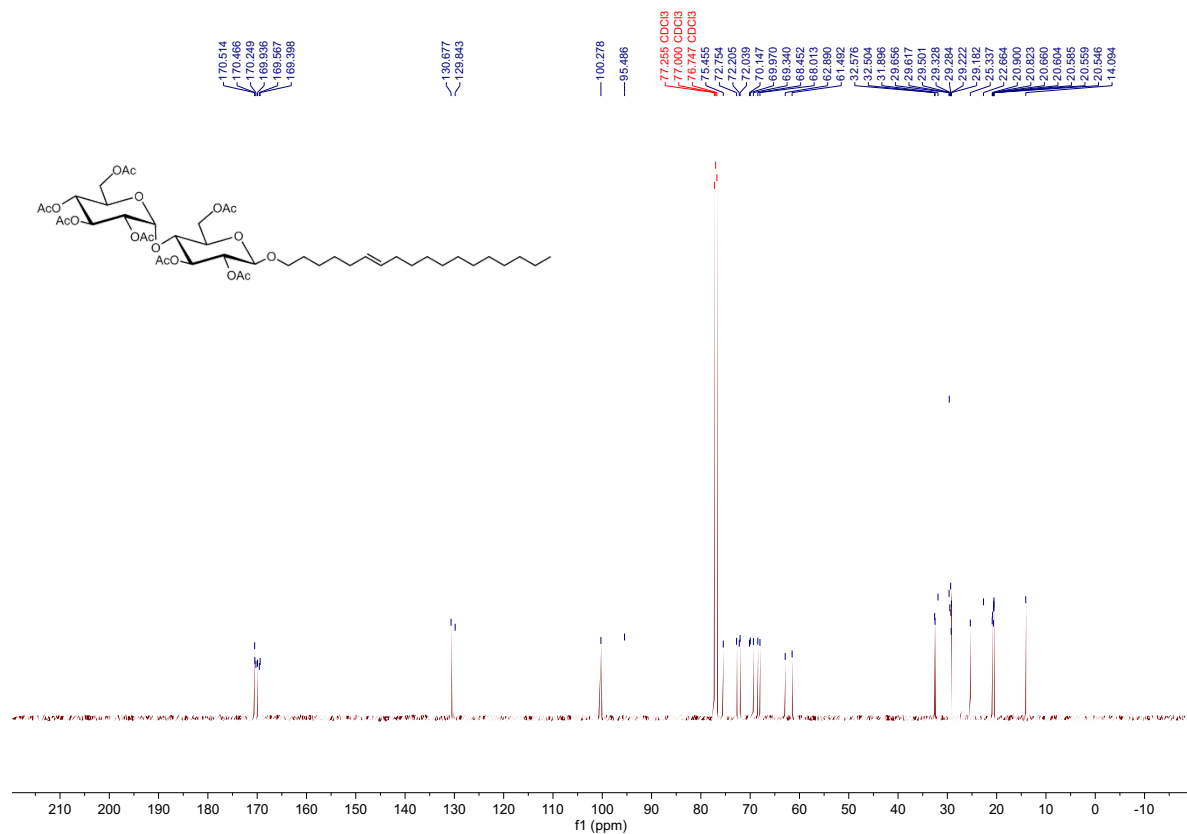


Fig. S2. ^{13}C NMR spectrum of *O*-(*E*-6-octadecenyl) hepta-acetyl-maltose.

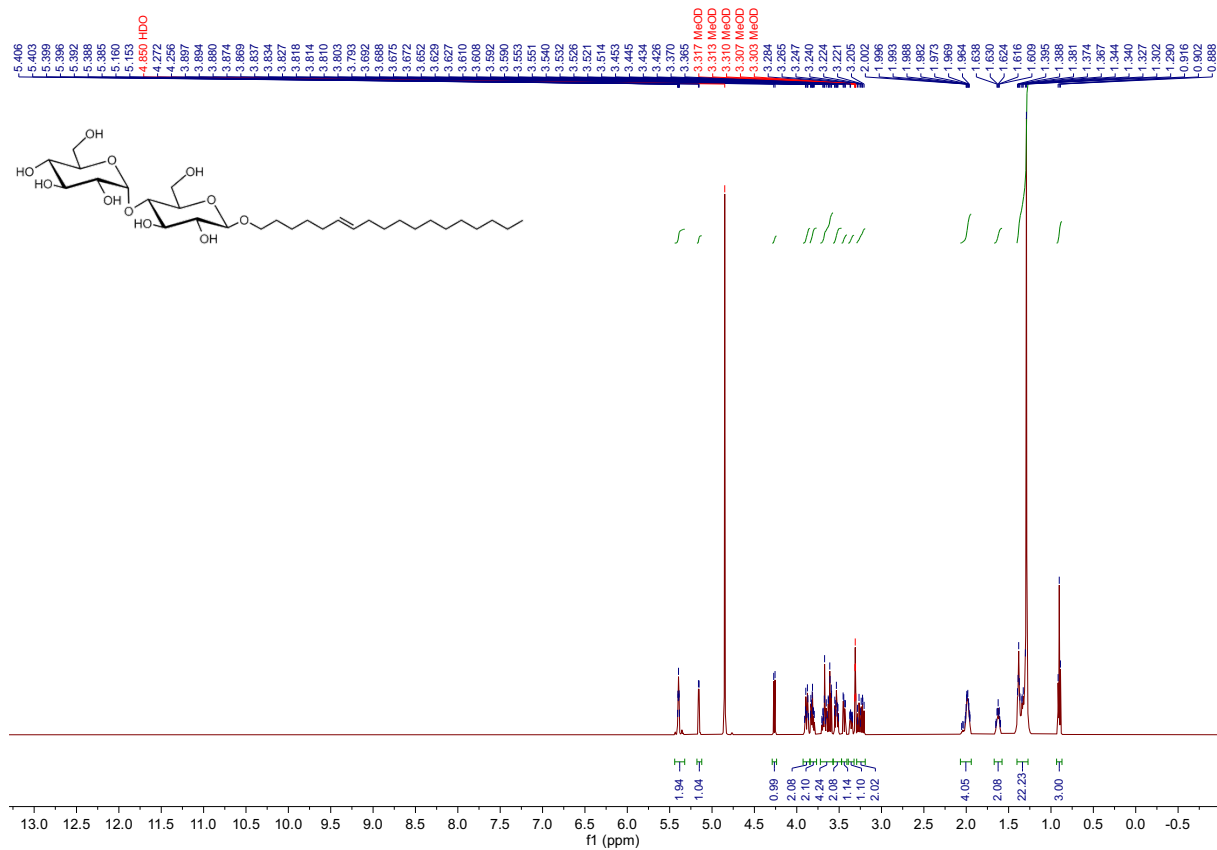


Fig. S3. ¹H NMR spectrum of *O*-(*E*-6-octadecenyl)-β-D-maltopyranoside

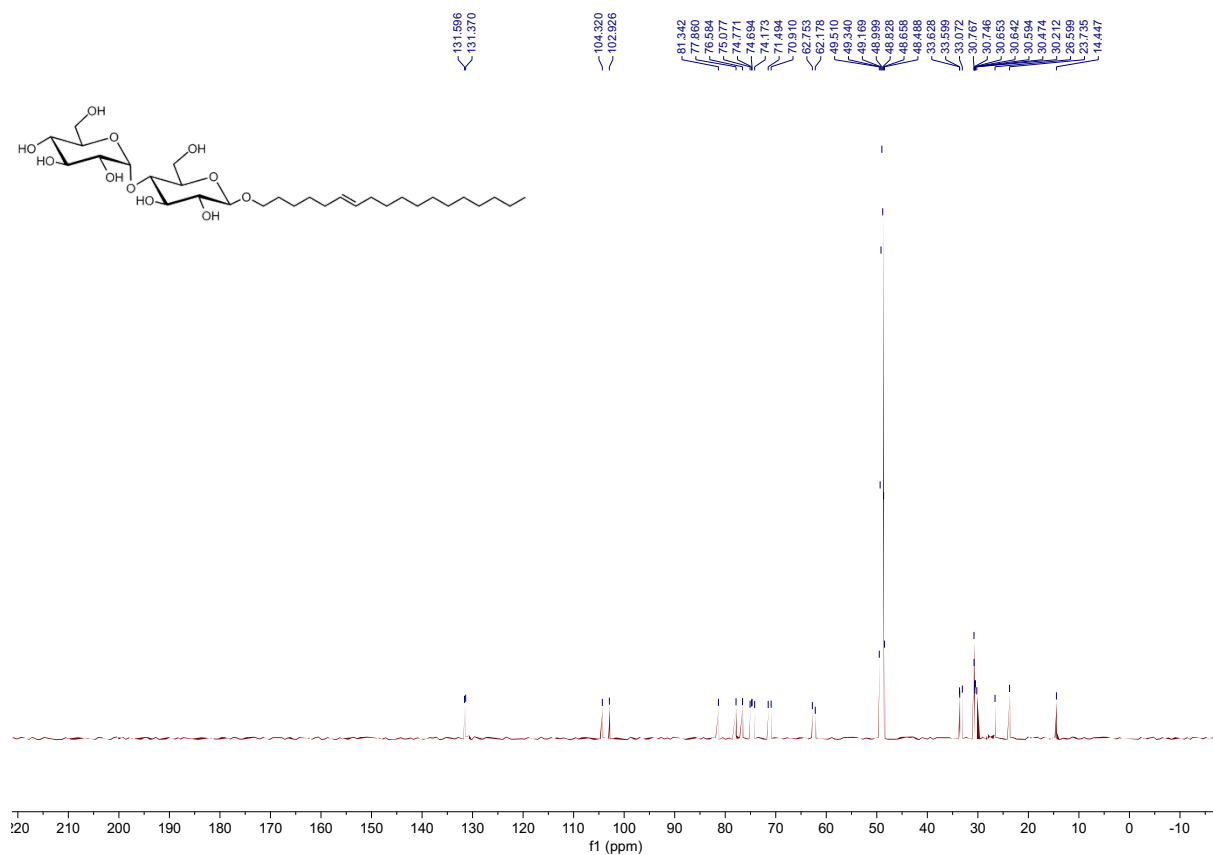


Fig. S4. ¹³C NMR spectrum of *O*-(*E*-6-octadecenyl)-β-D-maltopyranoside.

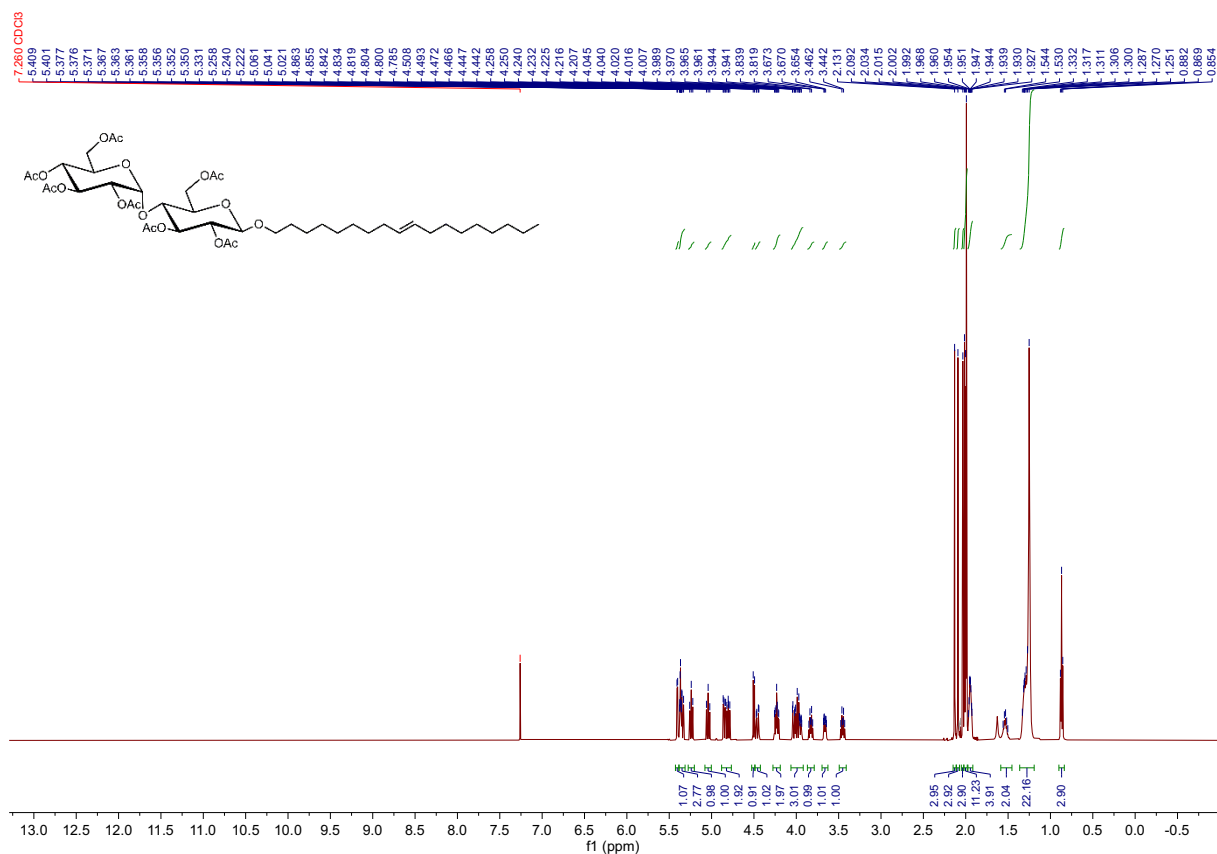


Fig. S5. $^1\text{H NMR}$ spectrum of *O*-(*E*-9-octadecenyl) hepta-acetyl-maltose.

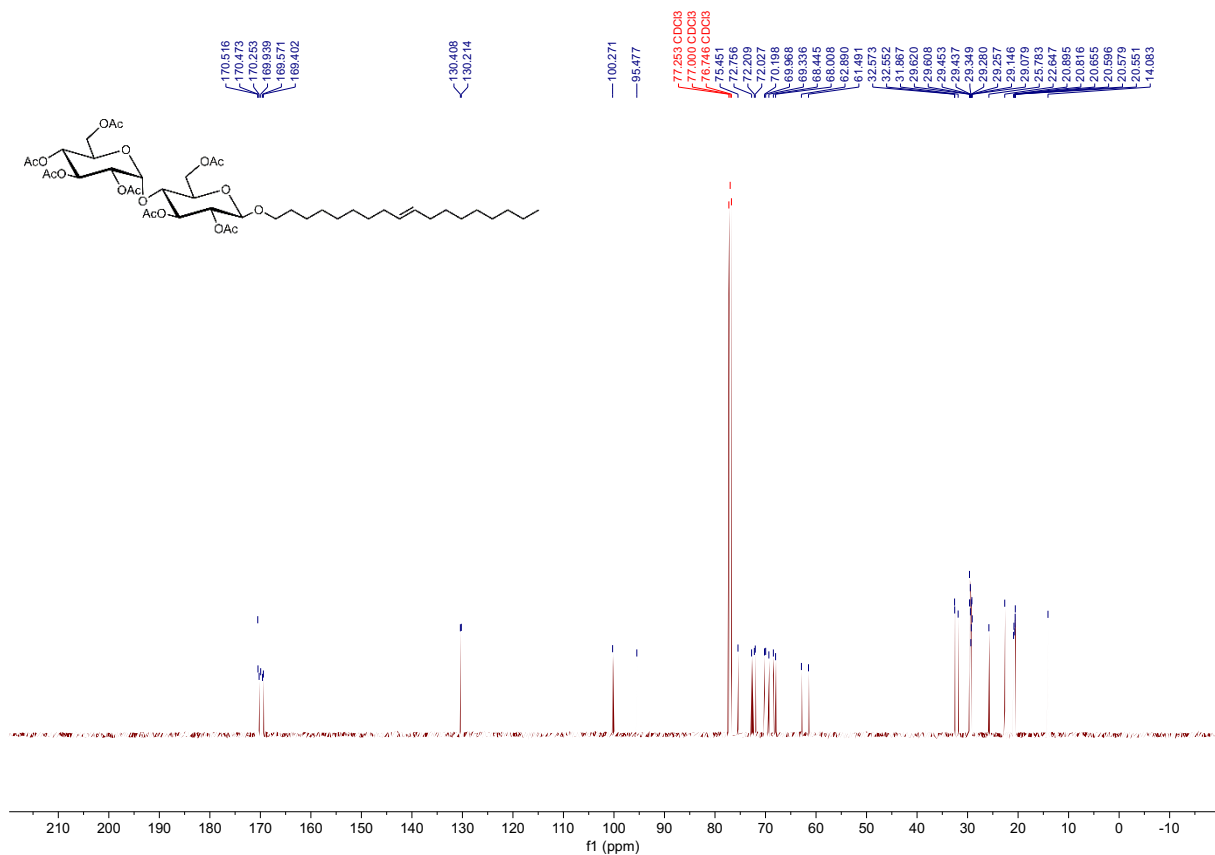


Fig. S6. $^{13}\text{C NMR}$ spectrum of *O*-(*E*-9-octadecenyl) hepta-acetyl-maltose.

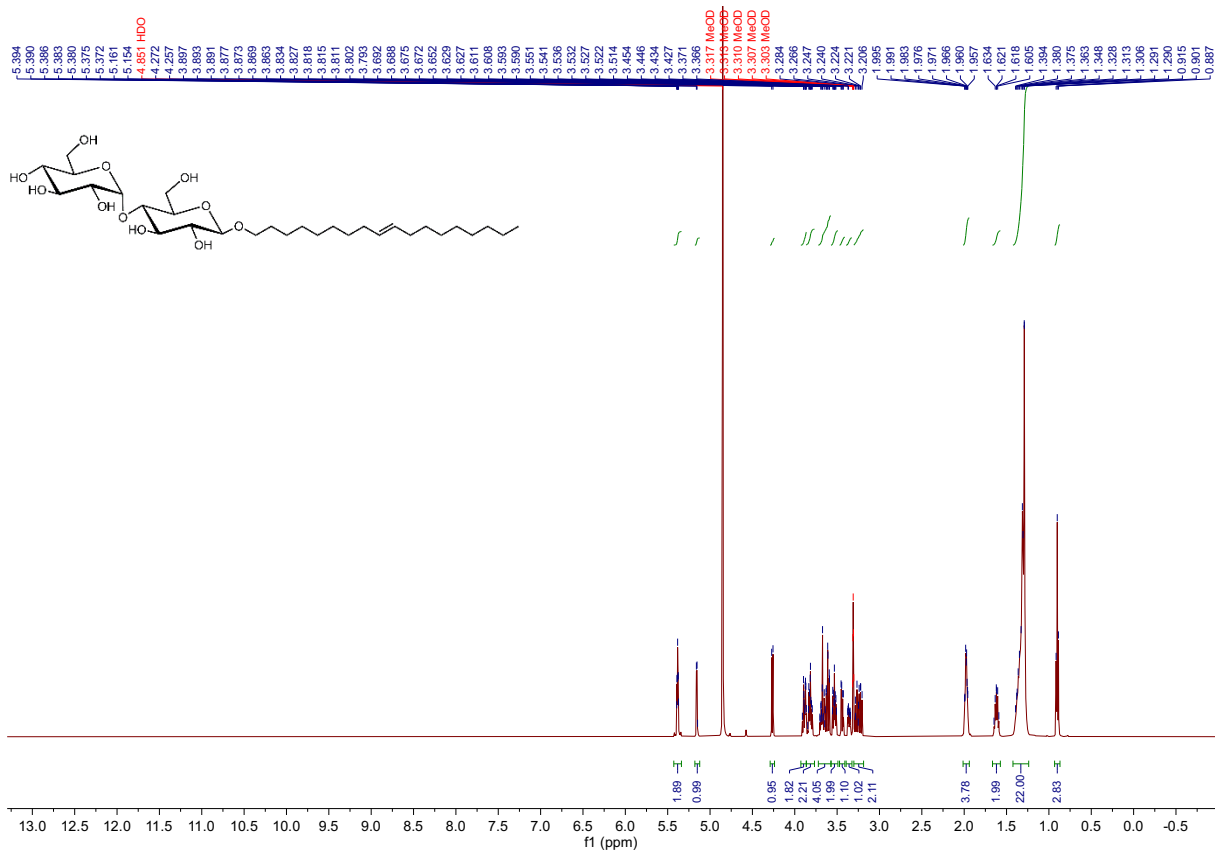


Fig. S7. ¹H NMR spectrum of *O*-(*E*-9-octadecenyl)-β-D-maltopyranoside

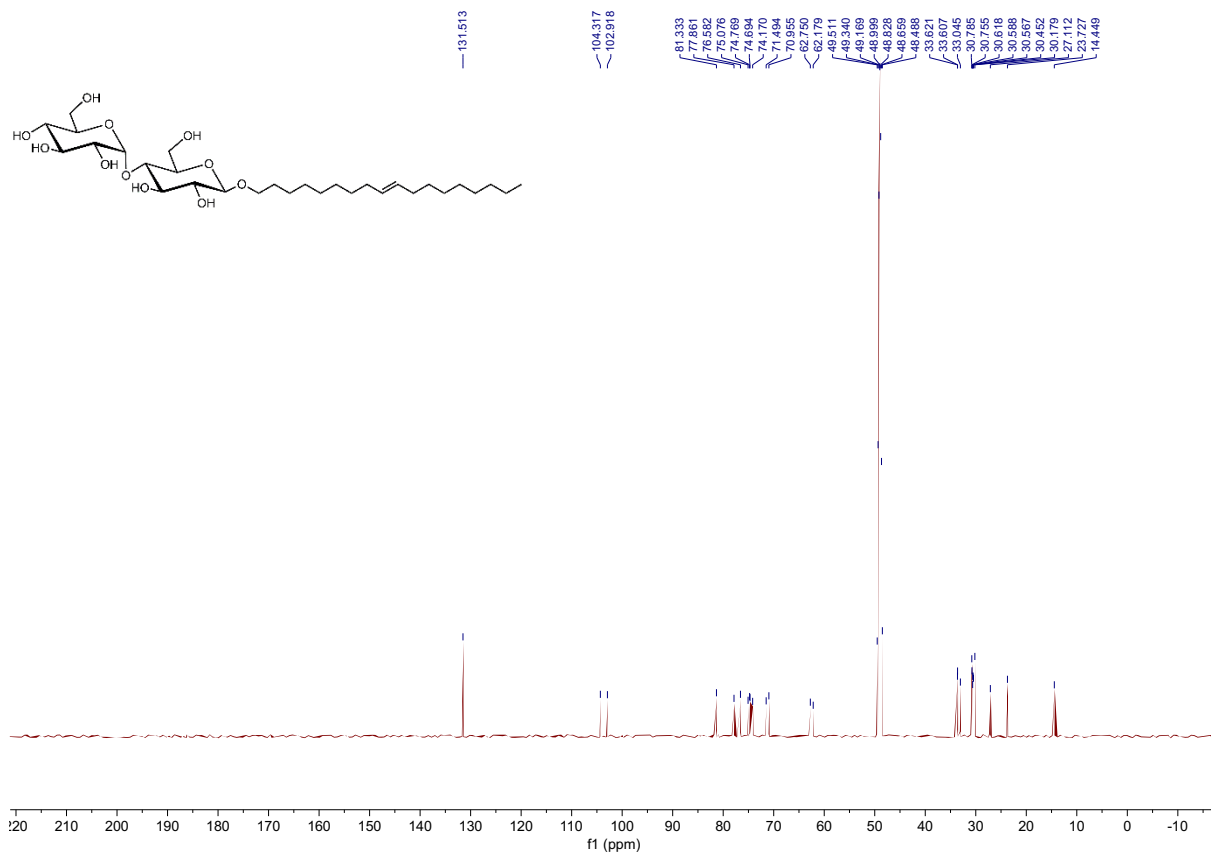


Fig. S8. ¹³C NMR spectrum of *O*-(*E*-9-octadecenyl)-β-D-maltopyranoside.

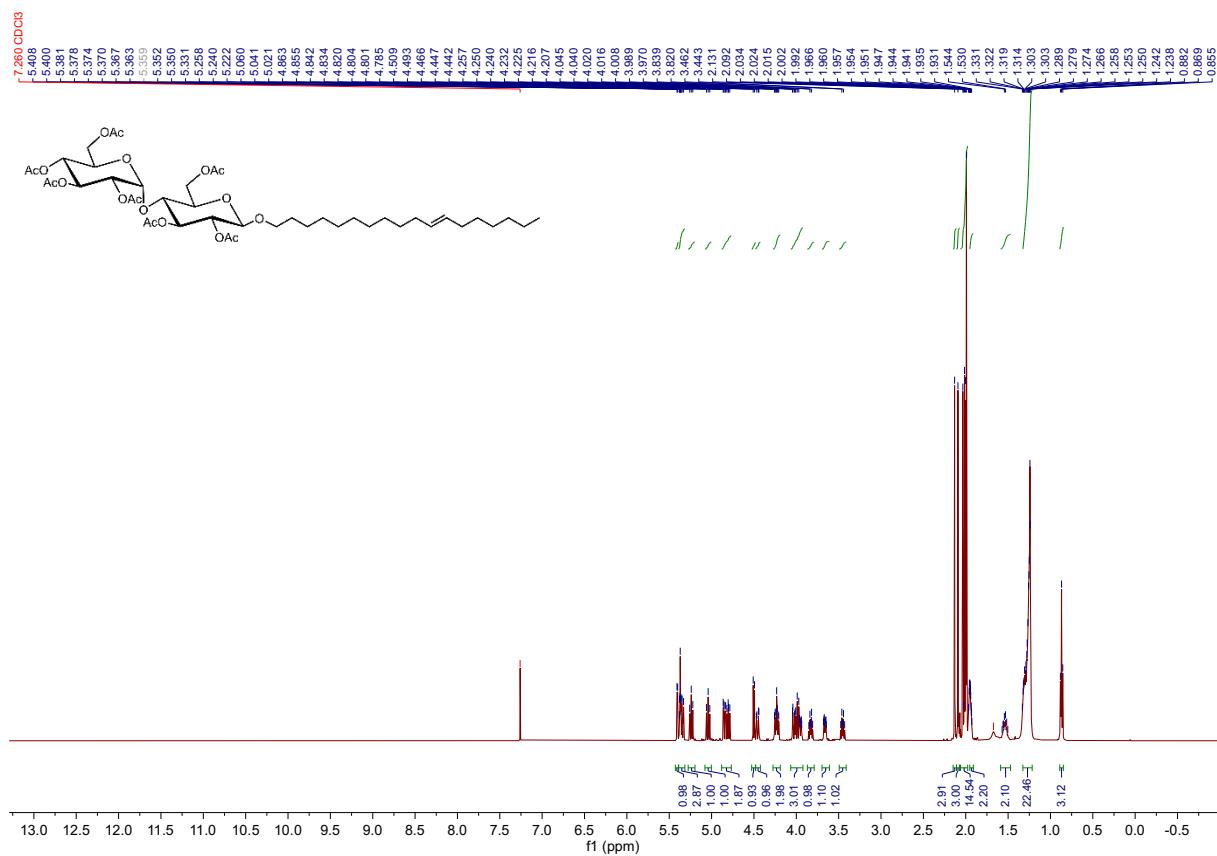


Fig. S9. ^1H NMR spectrum of *O*-(*E*-11-octadecenyl) hepta-acetyl-maltose.

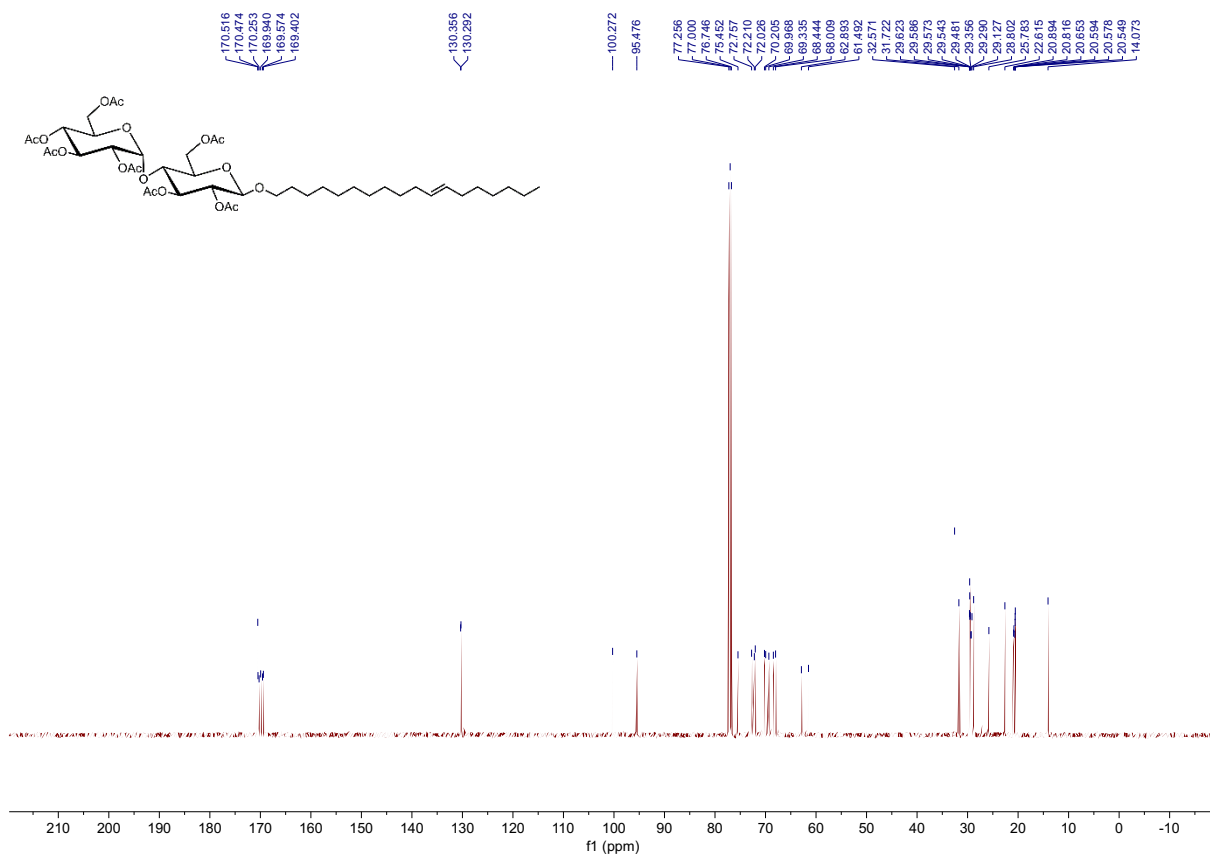


Fig. S10. ^{13}C NMR spectrum of *O*-(*E*-11-octadecenyl) hepta-acetyl-maltose.

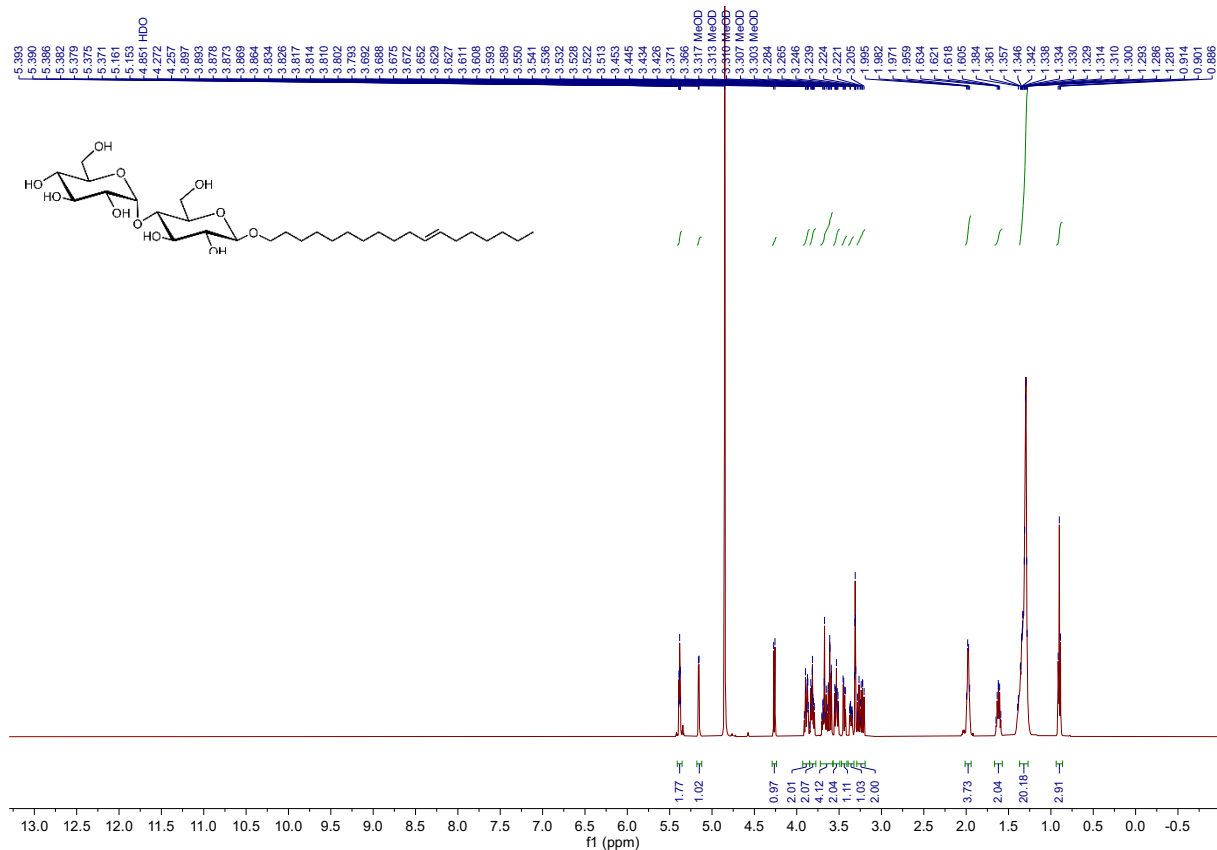


Fig. S11. ¹H NMR spectrum of *O*-(*E*-11-octadecenyl)-β-D-maltopyranoside

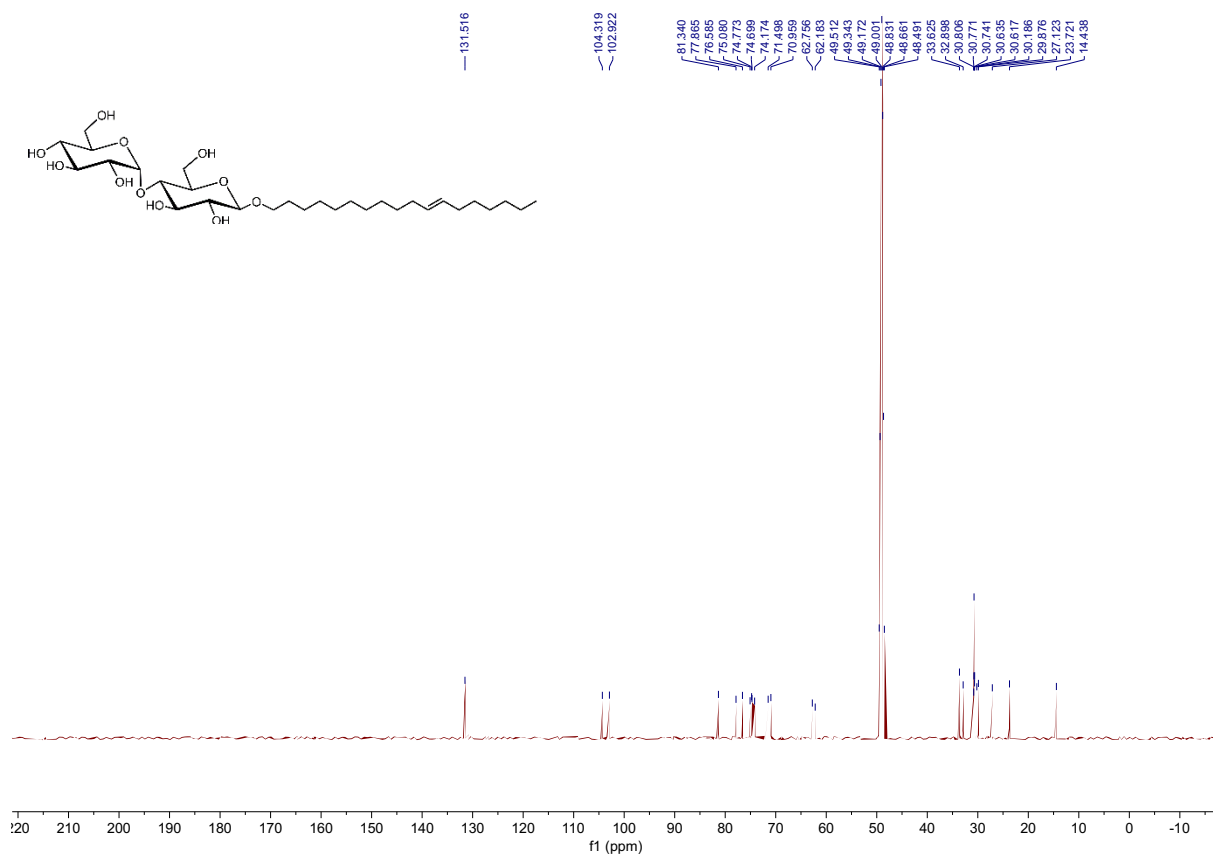


Fig. S12. ¹³C NMR spectrum of *O*-(*E*-11-octadecenyl)-β-D-maltopyranoside.

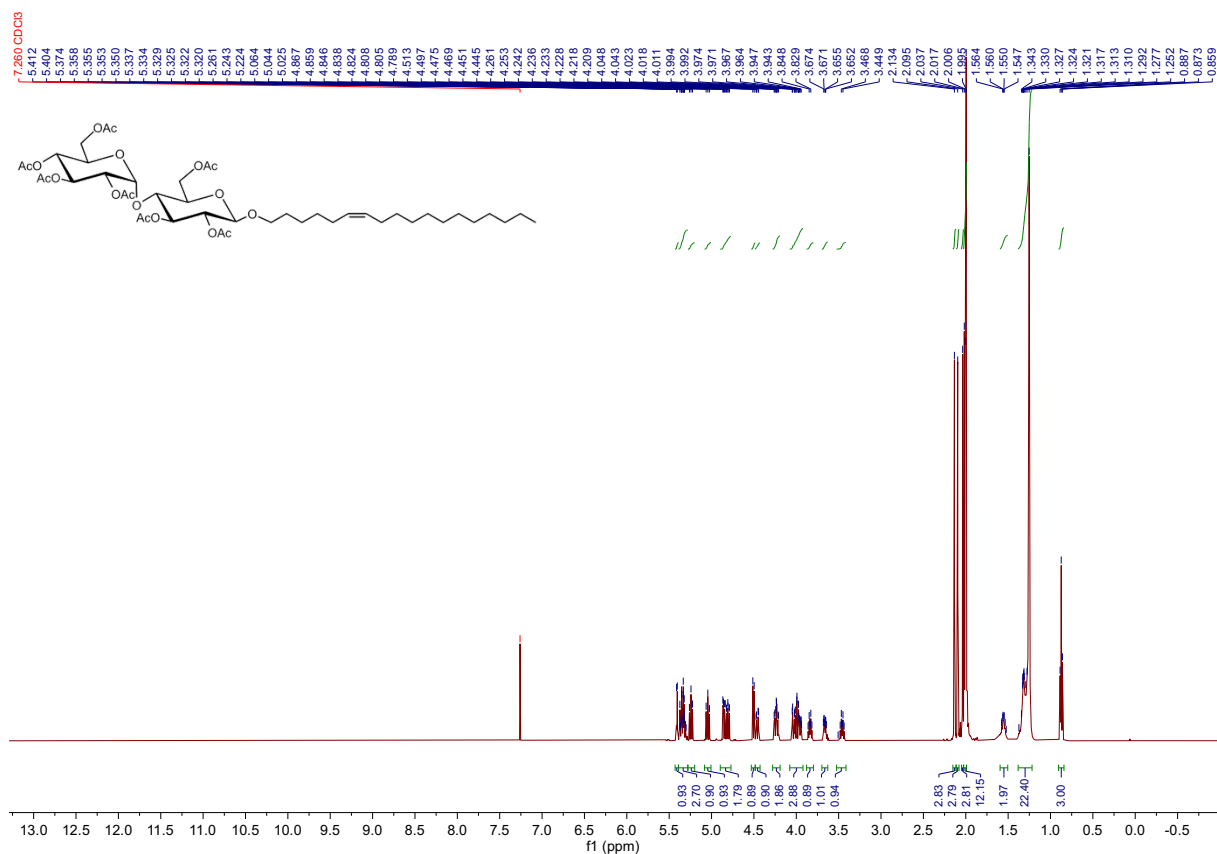


Fig. S13. ¹H NMR spectrum of *O*-(*Z*-6-octadecenyl) hepta-acetyl-maltose.

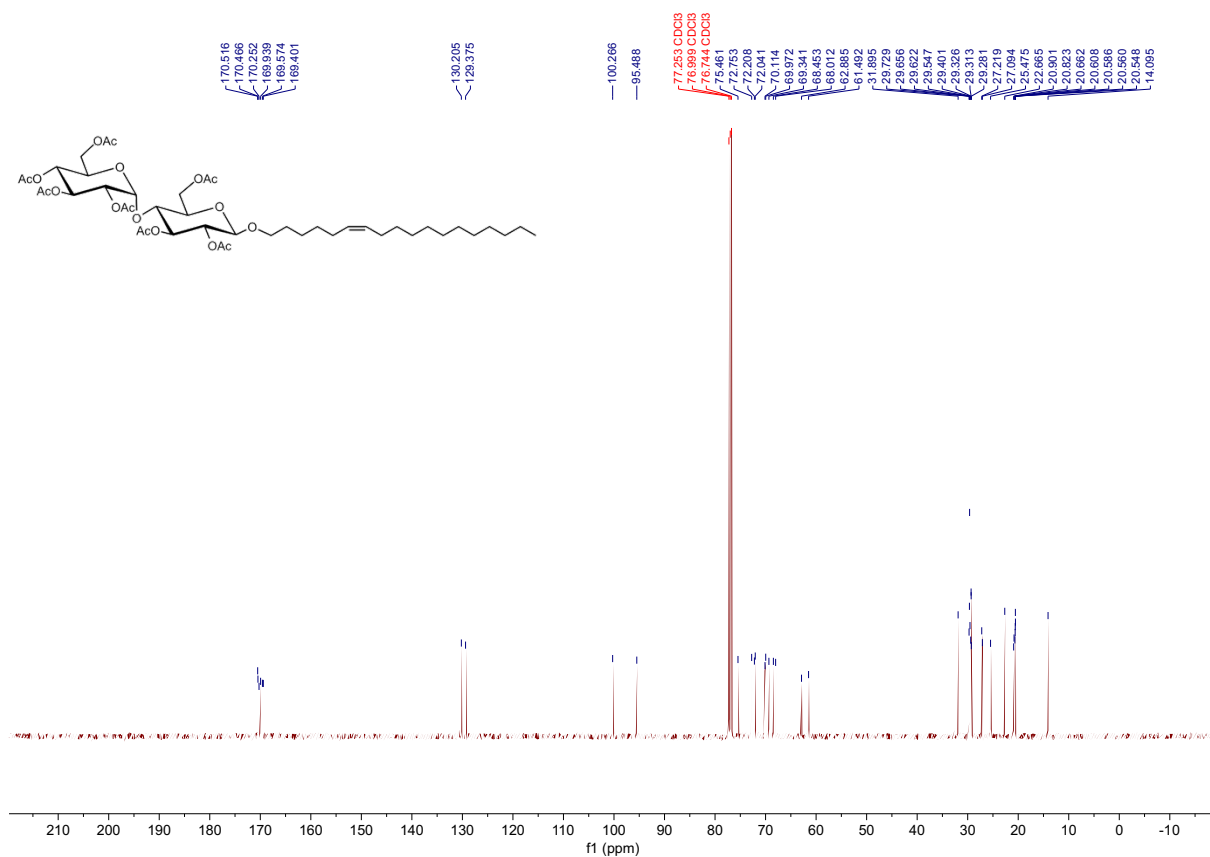


Fig. S14. ¹³C NMR spectrum of *O*-(*Z*-6-octadecenyl) hepta-acetyl-maltose.

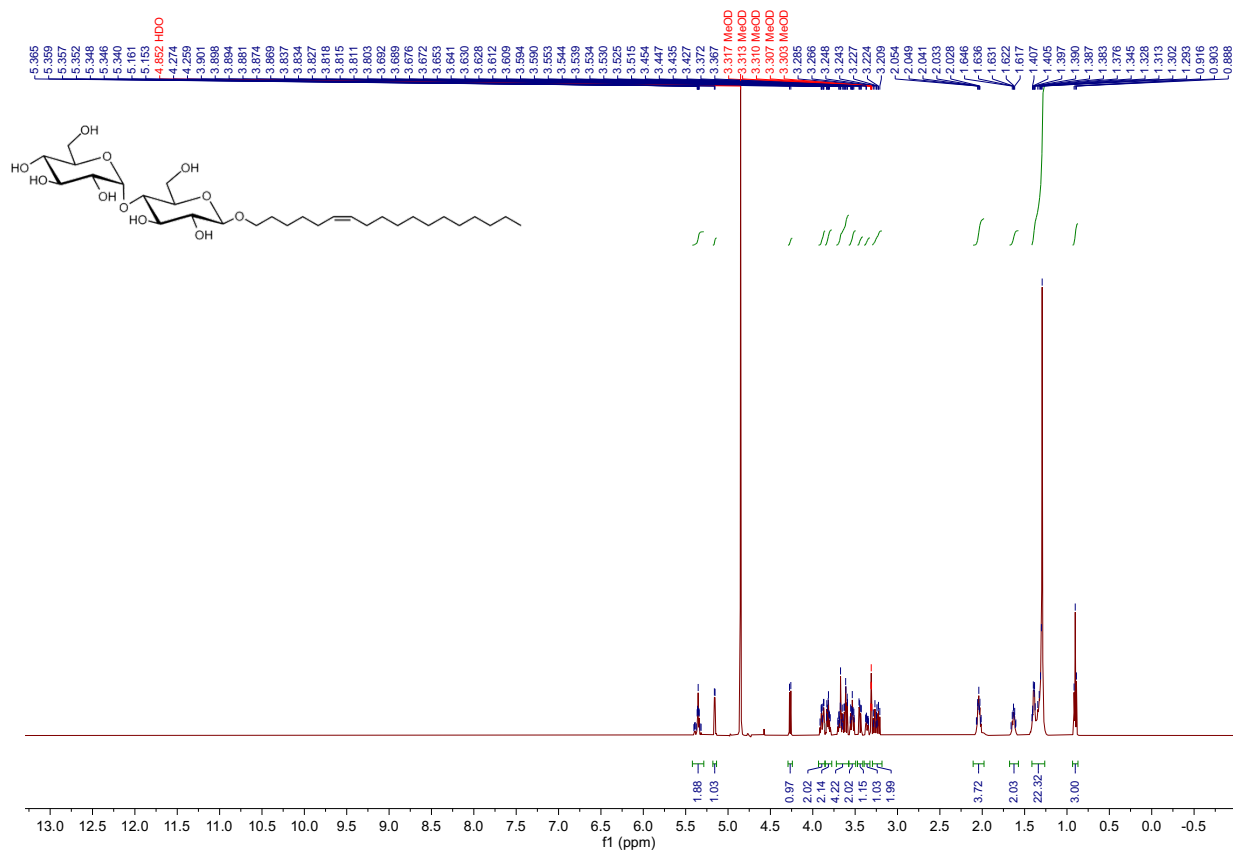


Fig. S15. ^1H NMR spectrum of *O*-(*Z*-6-octadecenyl)- β -D-maltopyranoside

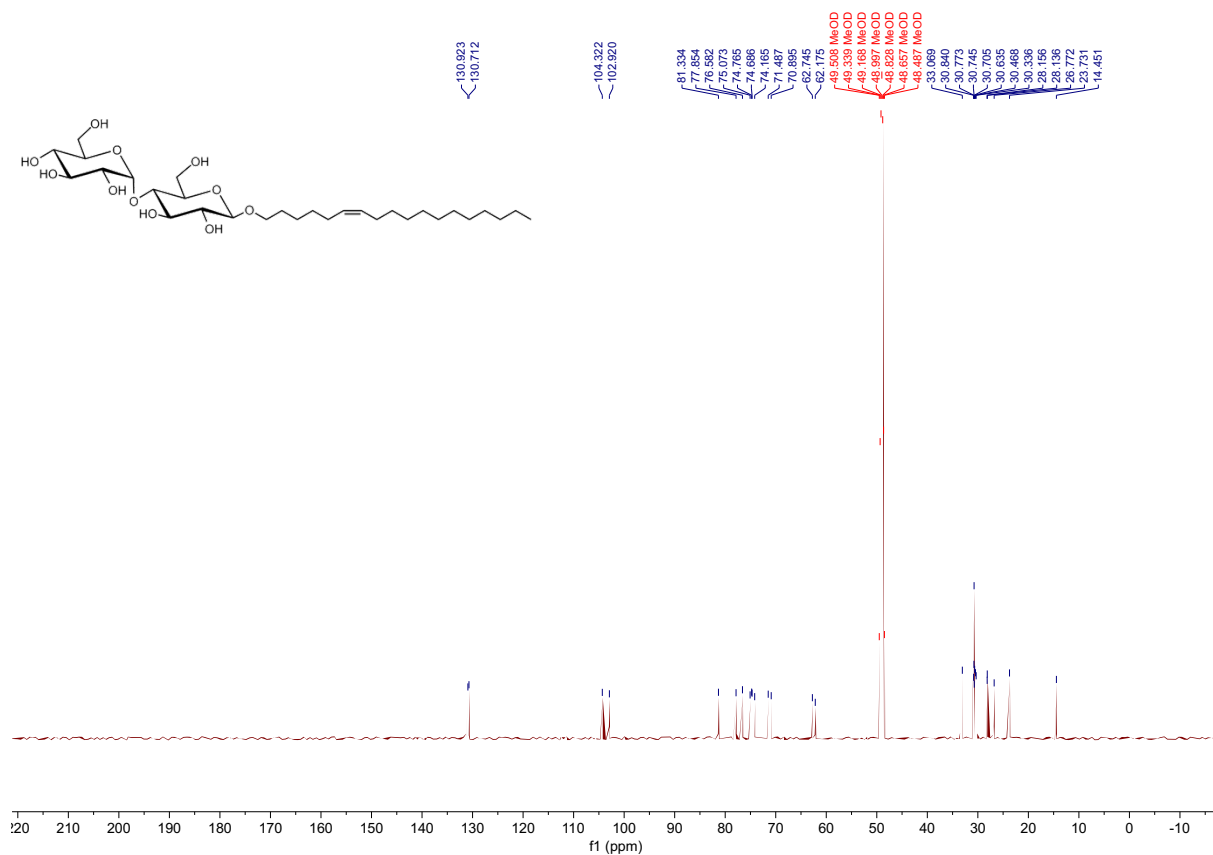


Fig. S16. ^{13}C NMR spectrum of *O*-(*Z*-6-octadecenyl)- β -D-maltopyranoside.

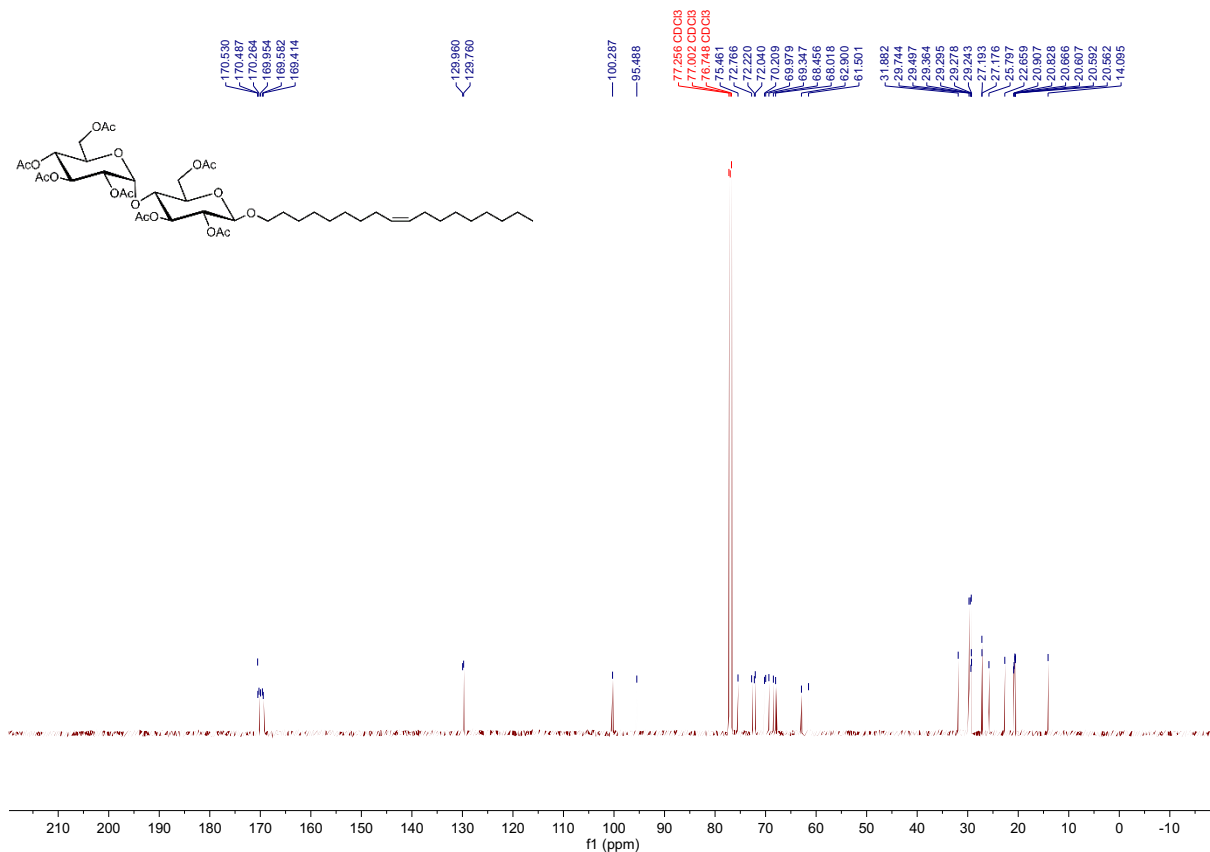


Fig. S17. ^1H NMR spectrum of *O*-(*Z*-9-octadecenyl) hepta-acetyl-maltose.

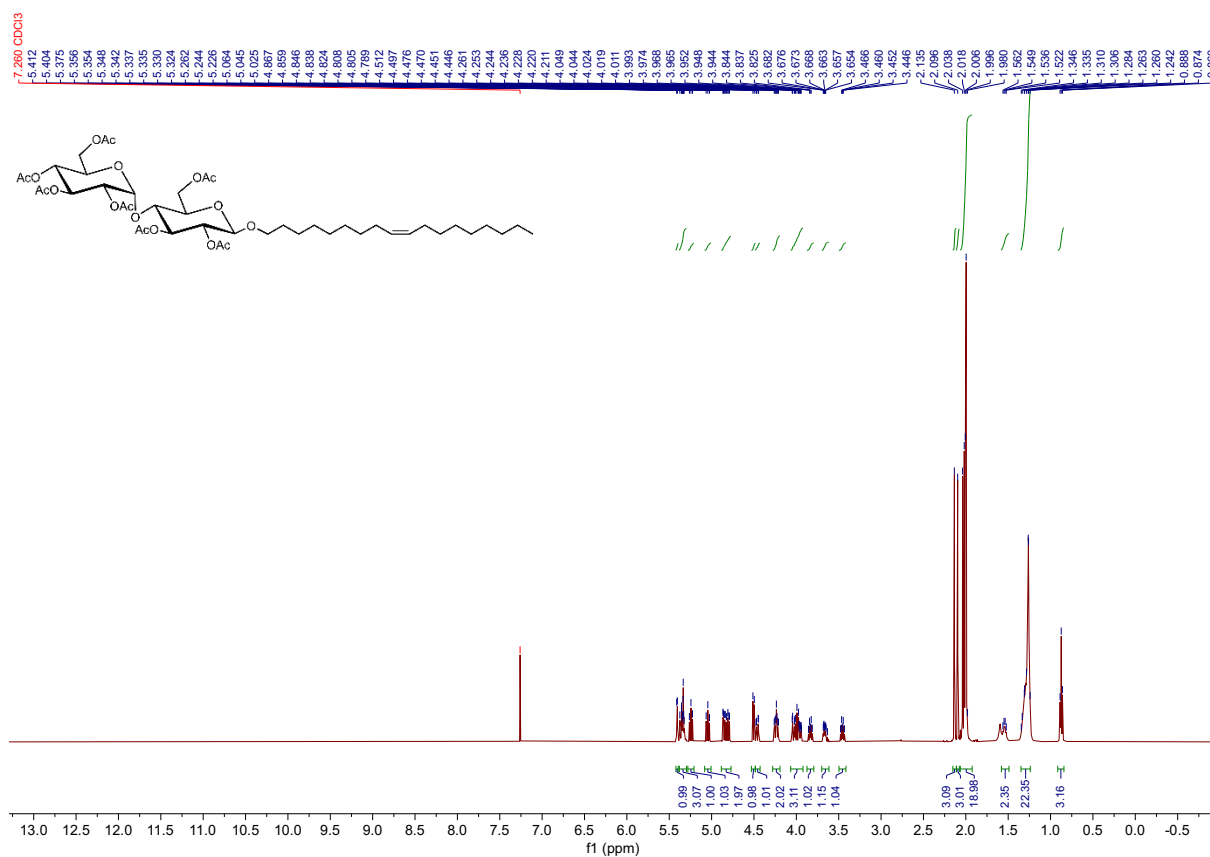


Fig. S18. ^{13}C NMR spectrum of *O*-(*Z*-9-octadecenyl) hepta-acetyl-maltose.

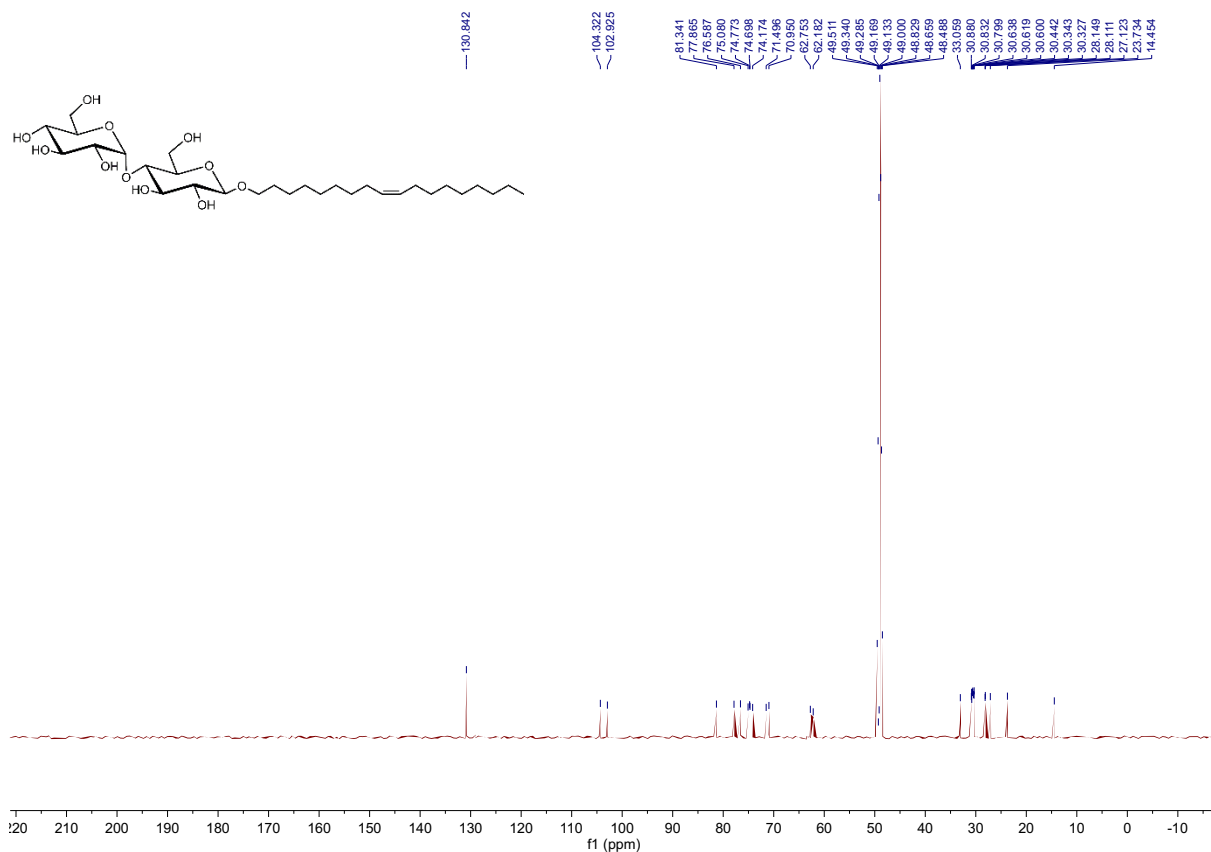


Fig. S19. ¹H NMR spectrum of *O*-(*Z*-9-octadecenyl)-β-D-maltopyranoside

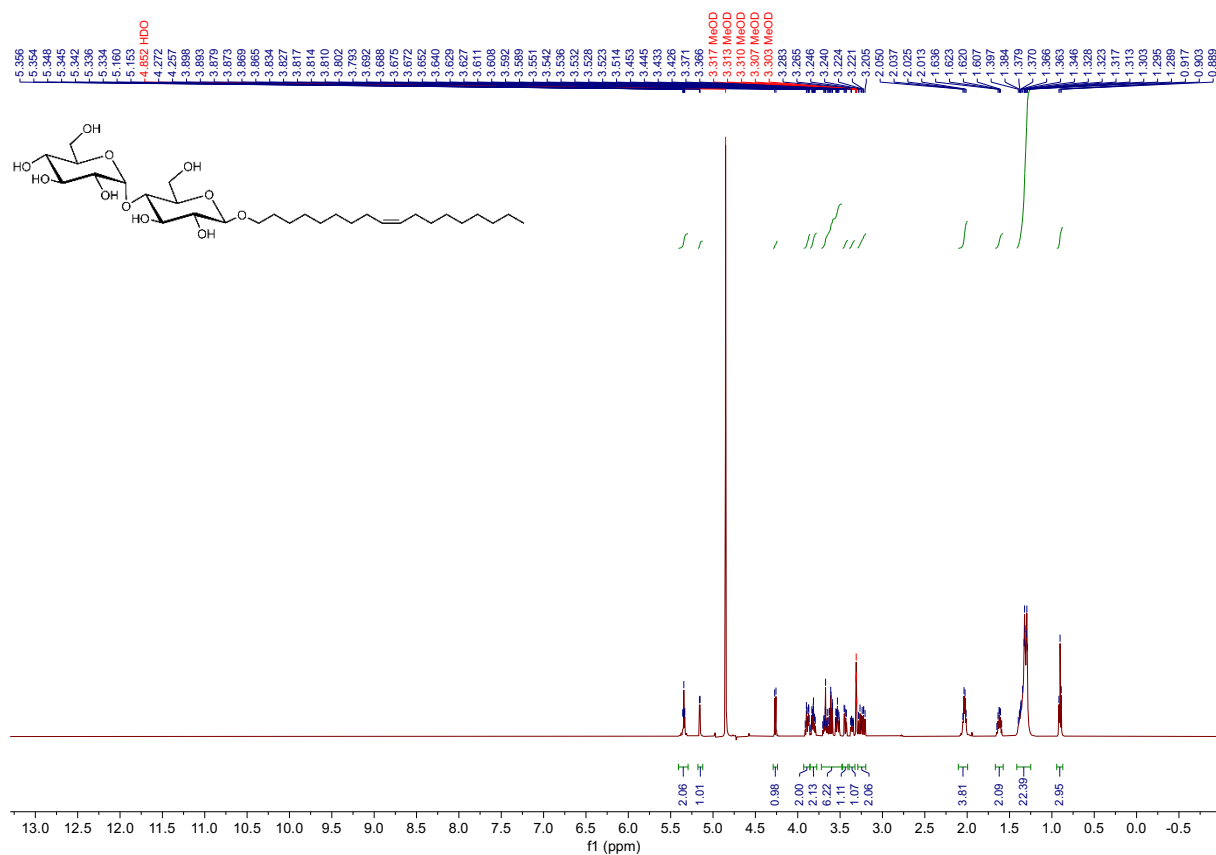


Fig. S20. ¹³C NMR spectrum of *O*-(*Z*-9-octadecenyl)-β-D-maltopyranoside.

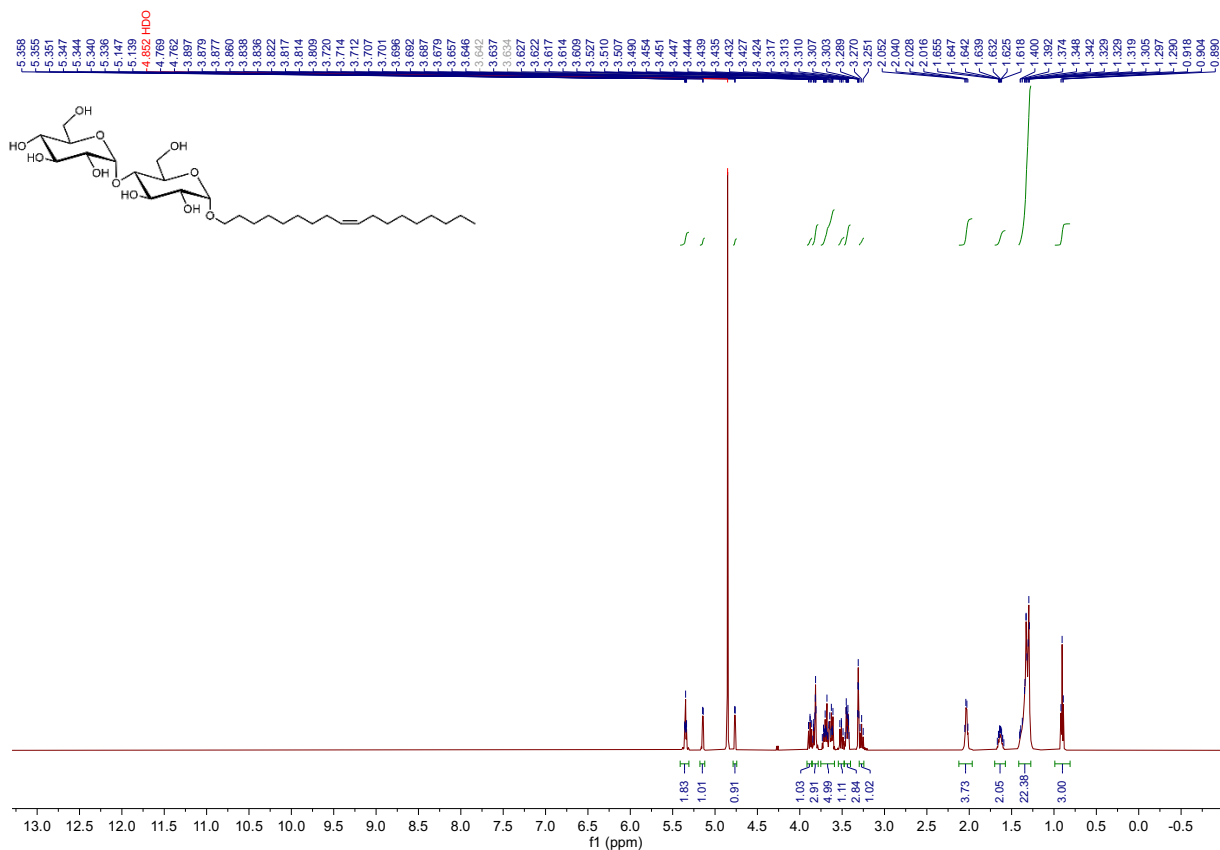


Fig. S21. ^1H NMR spectrum of *O*-(*Z*-9-octadecenyl)- α -D-maltopyranoside

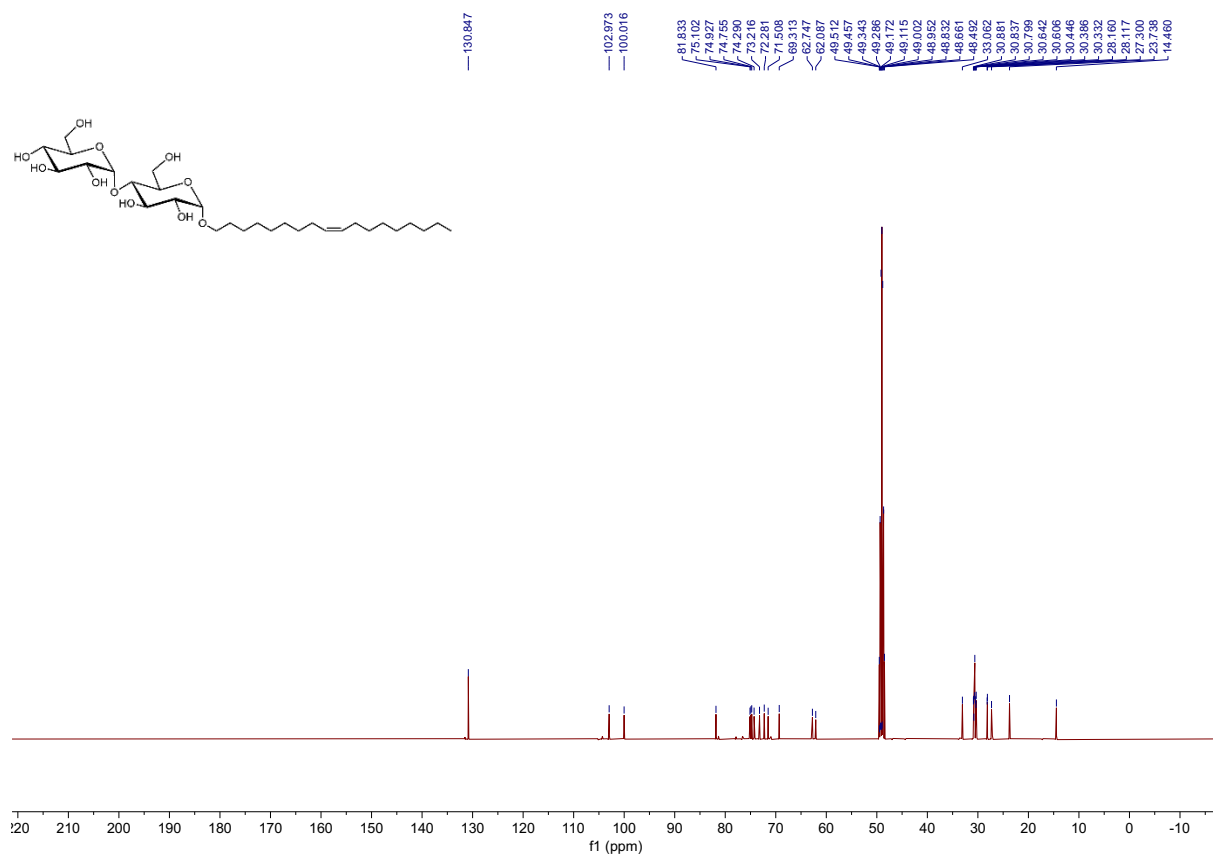


Fig. S22. ^{13}C NMR spectrum of *O*-(*Z*-9-octadecenyl)- α -D-maltopyranoside

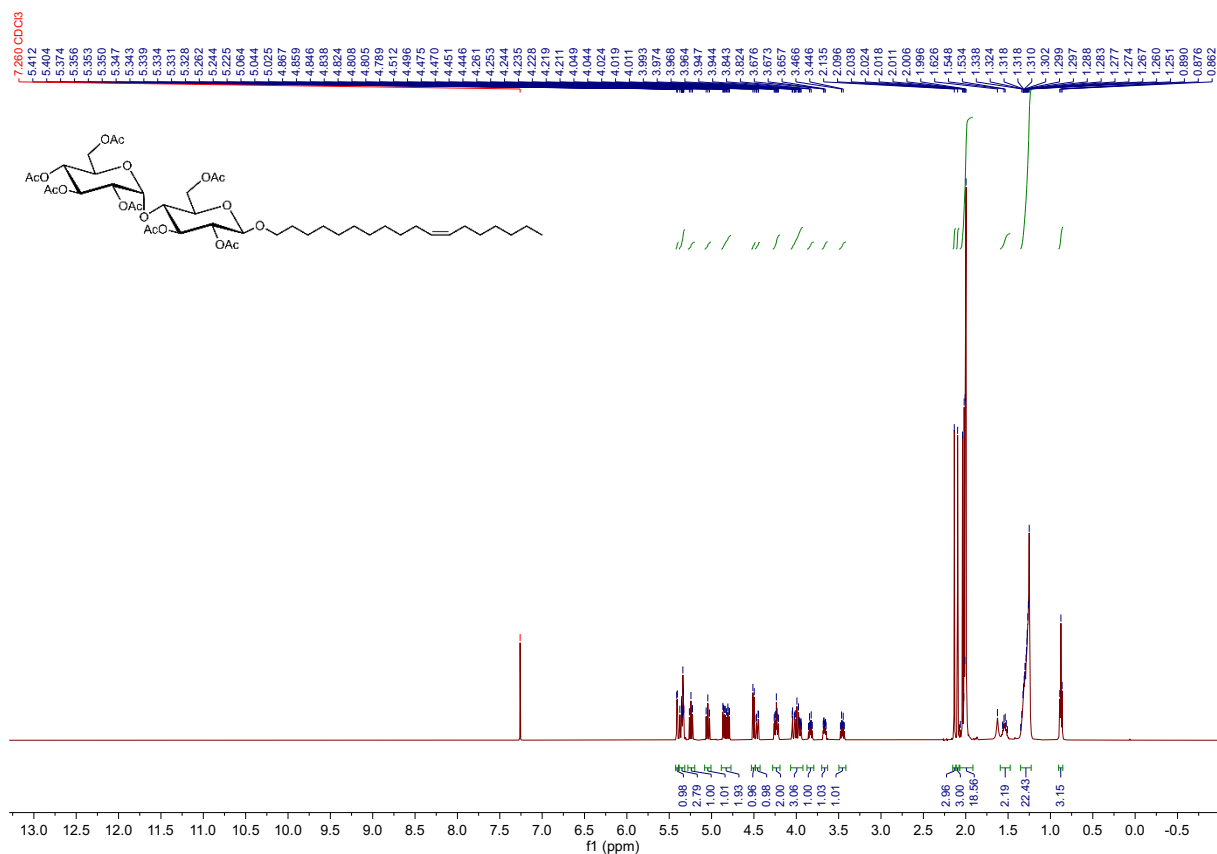


Fig. S23. ^1H NMR spectrum of *O*-(*Z*-11-octadecenyl) hepta-acetyl-maltose.

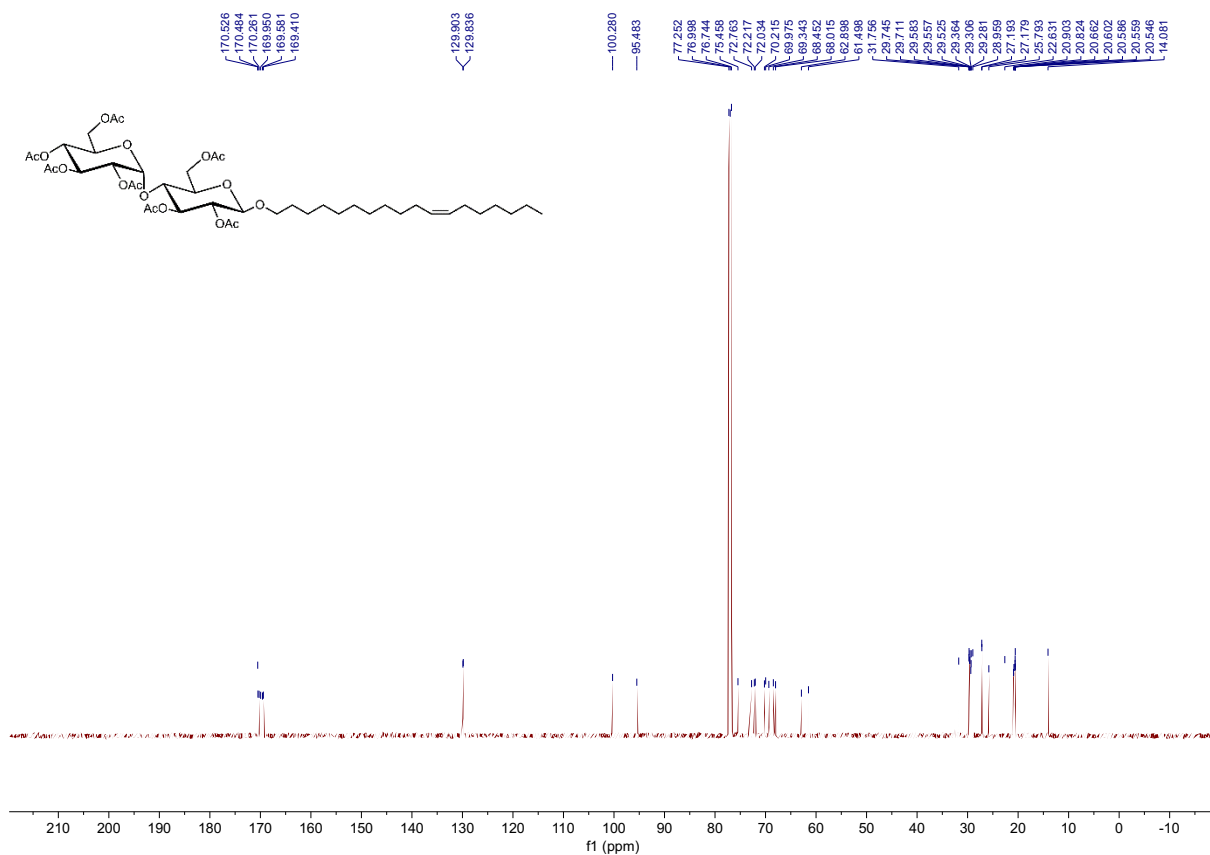


Fig. S24. ^{13}C NMR spectrum of *O*-(*Z*-11-octadecenyl) hepta-acetyl-maltose.

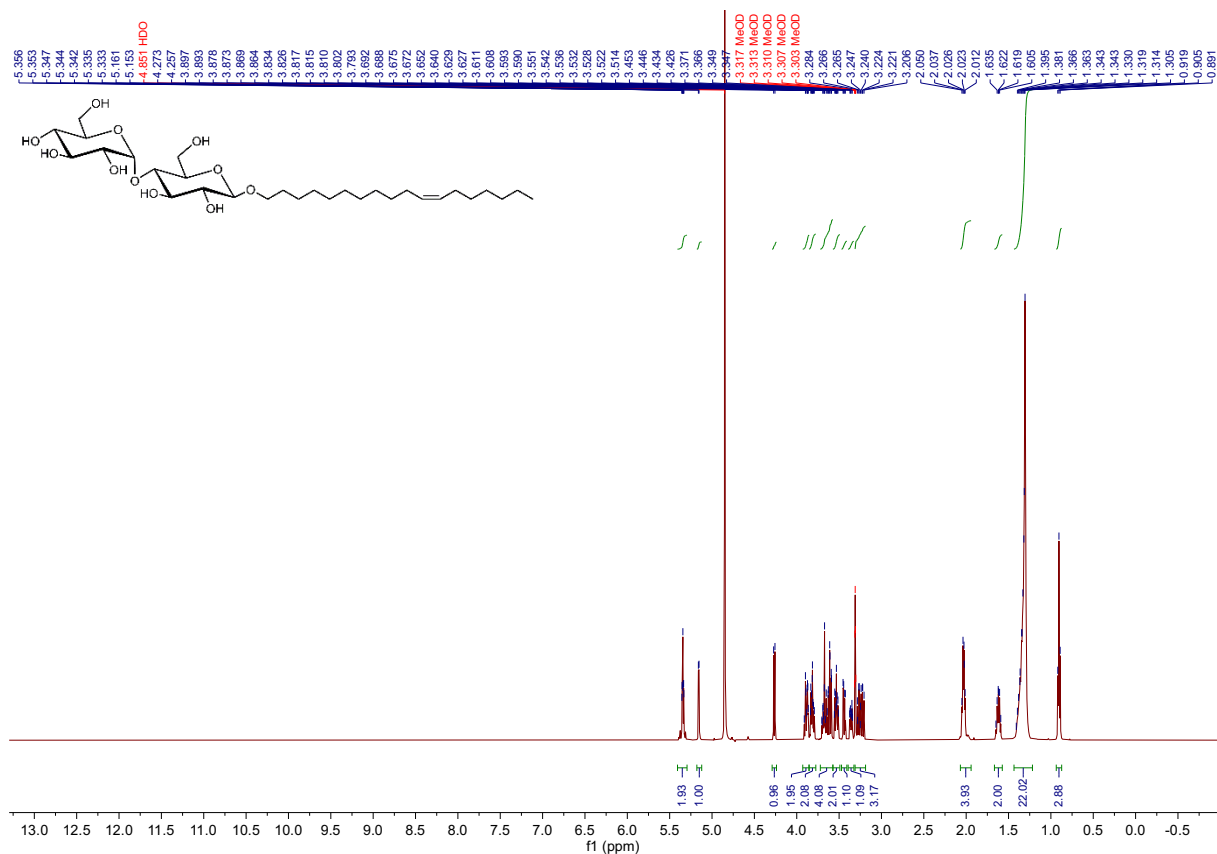


Fig. S25. ¹H NMR spectrum of *O*-(*Z*-11-octadecenyl)-β-D-maltopyranoside

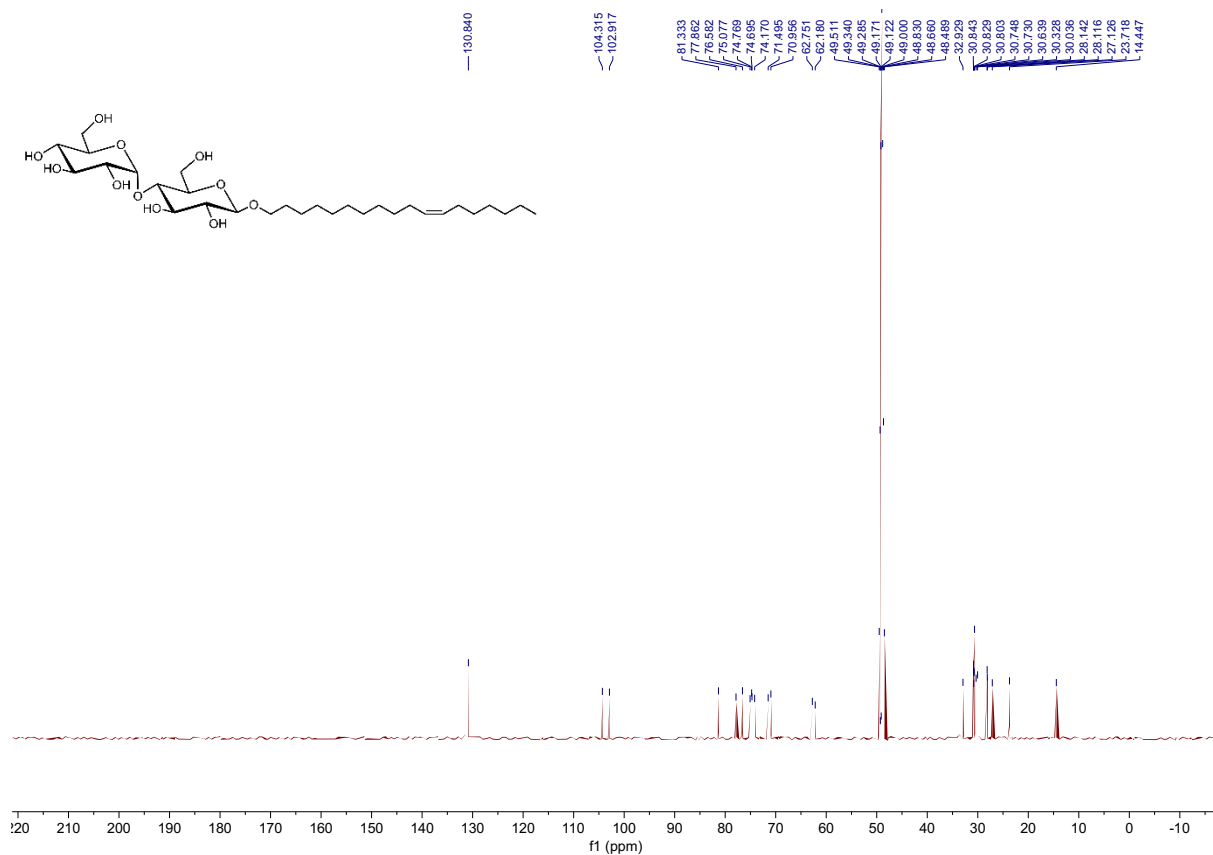


Fig. S26. ¹³C NMR spectrum of *O*-(*Z*-11-octadecenyl)-β-D-maltopyranoside.

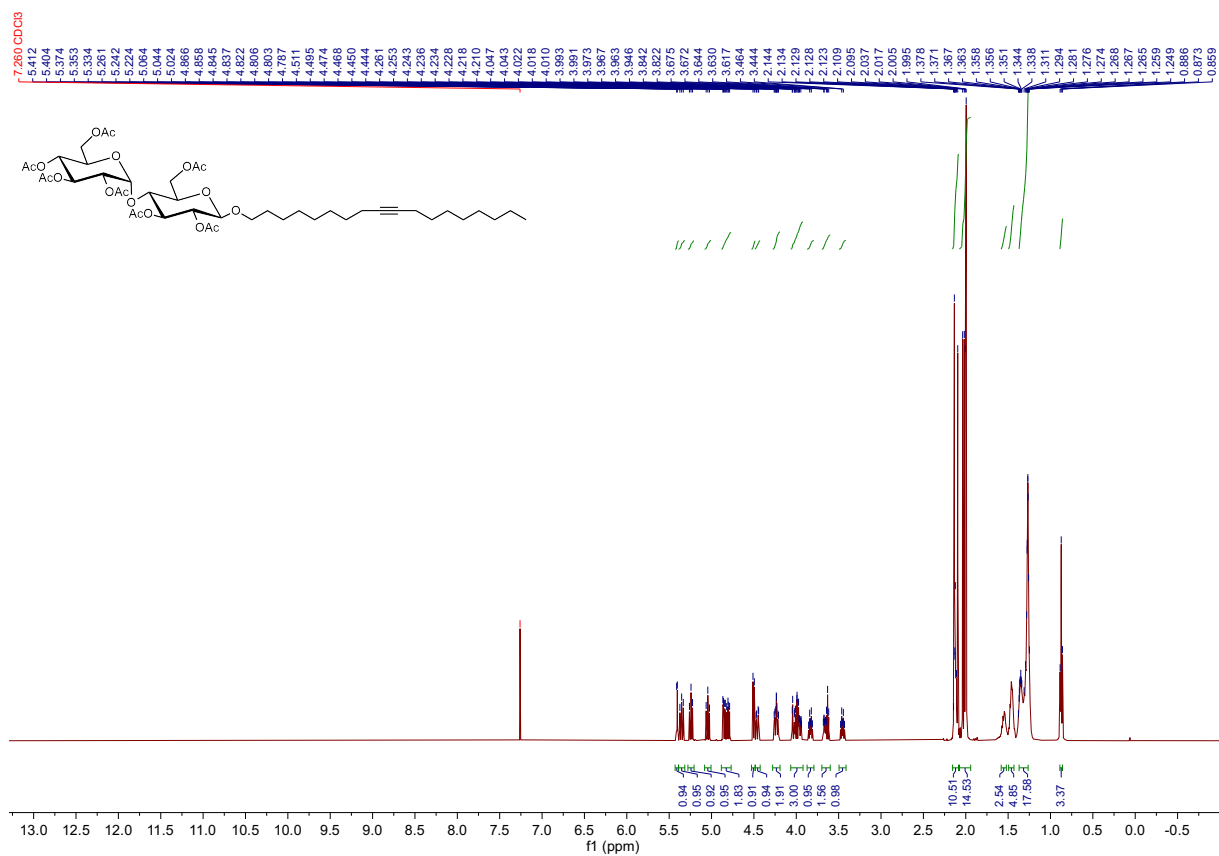


Fig. S27. ¹H NMR spectrum of *O*-(9-octadecynyl)-hepta-acetyl-maltose.

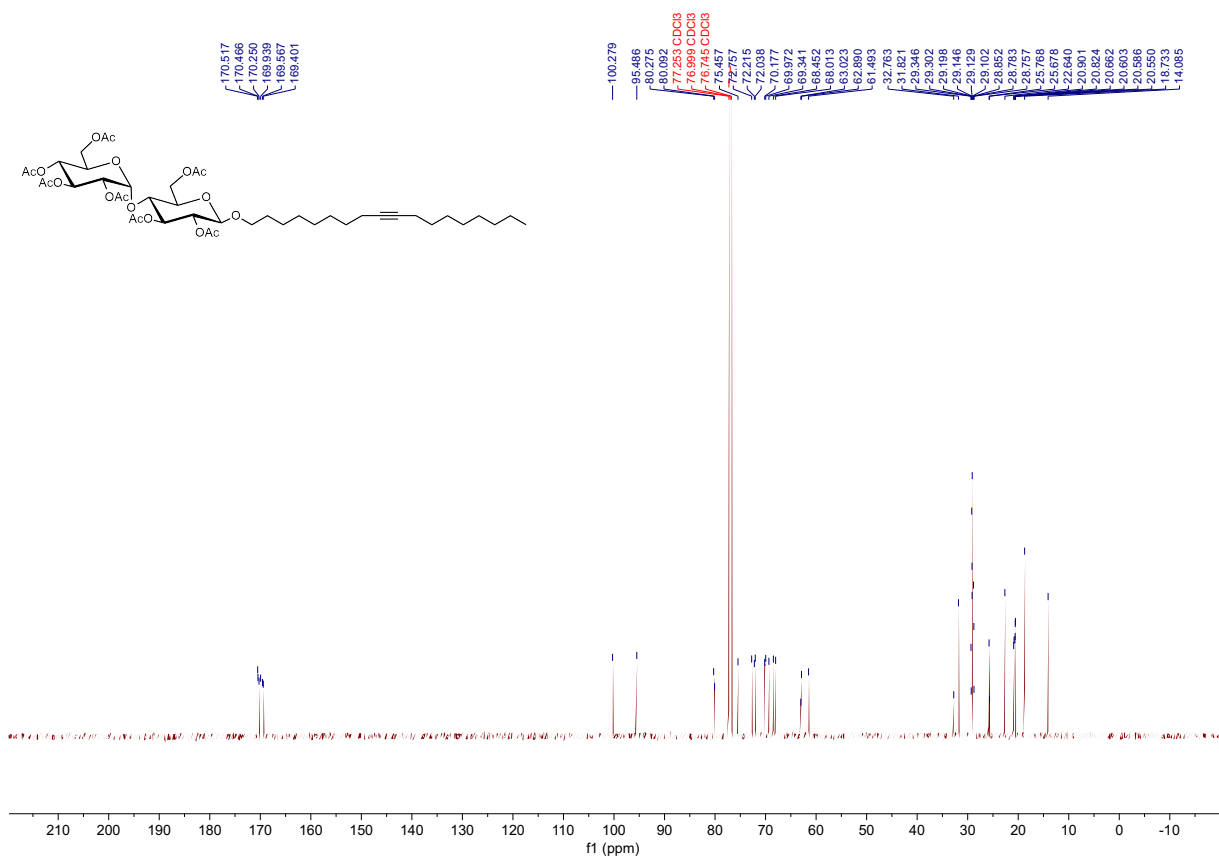


Fig. S28. ¹³C NMR spectrum of *O*-(9-octadecynyl)-hepta-acetyl-maltose.

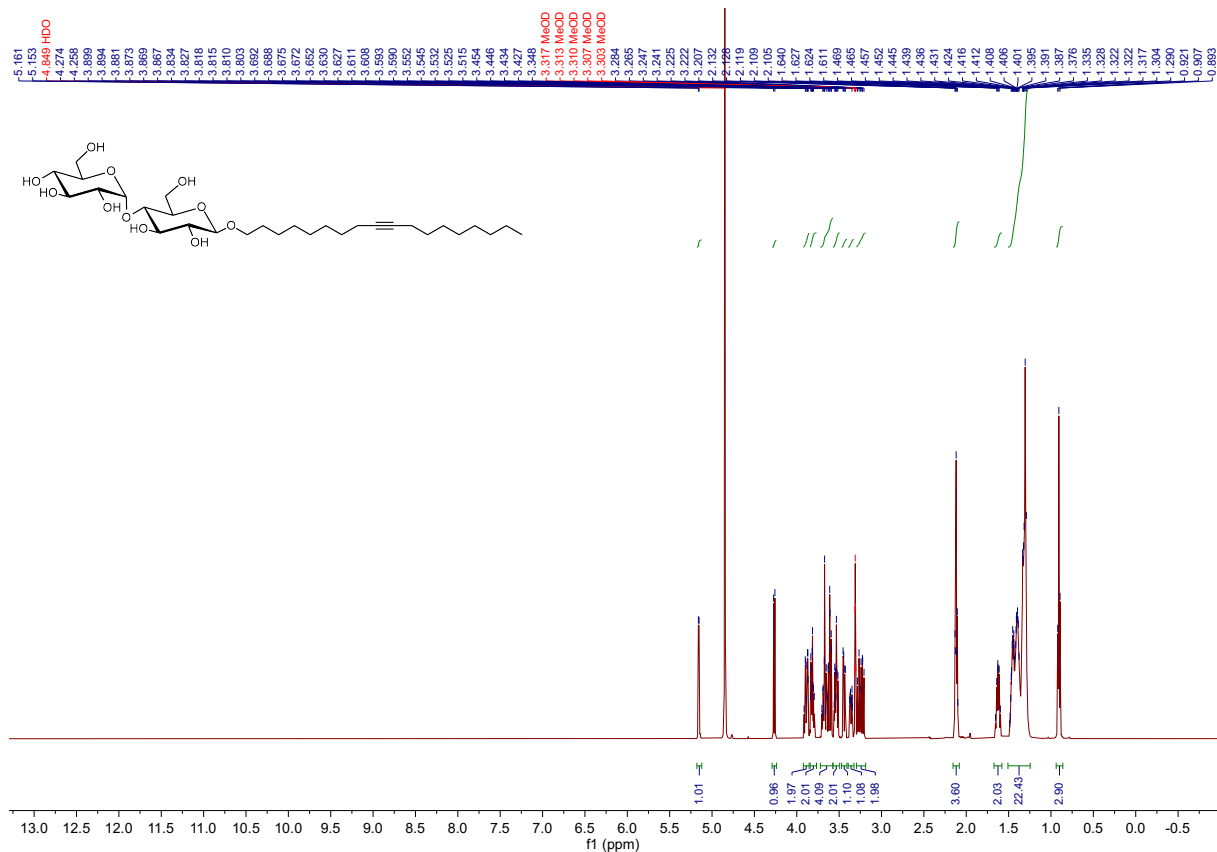


Fig. S29. ¹H NMR spectrum of (9-octadecynyl)-β-D-maltopyranoside.

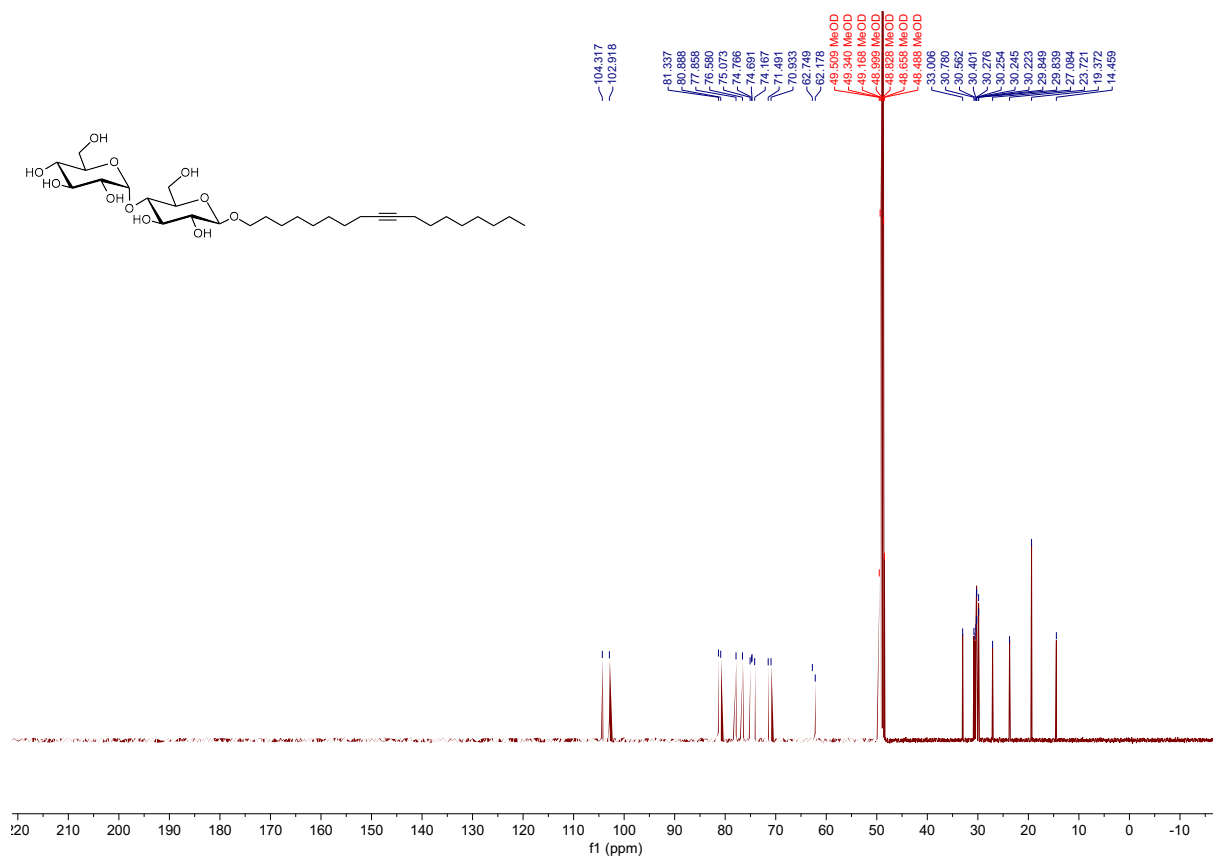


Fig. S30. ¹³C NMR spectrum of (9-octadecynyl)-β-D-maltopyranoside.

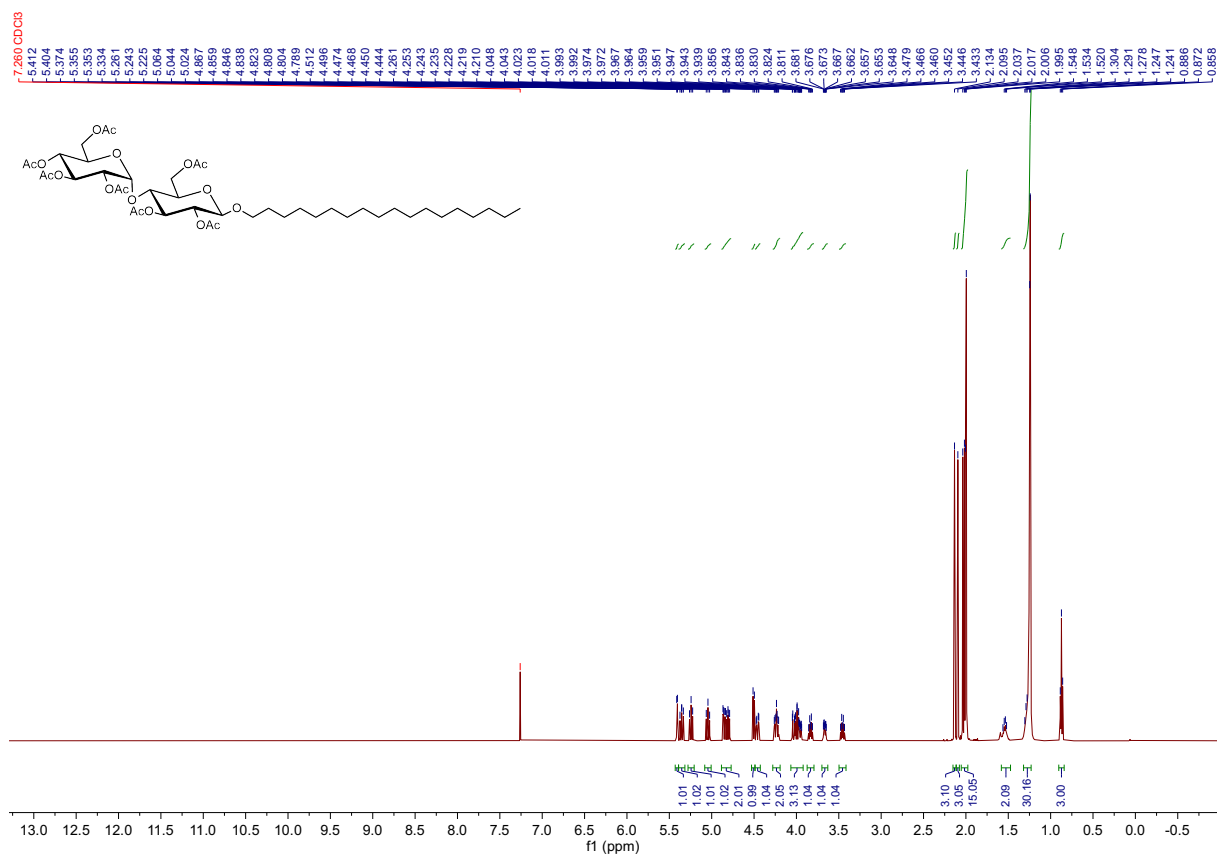


Fig. S31. ¹H NMR spectrum of *O*-(octadecyl)-hepta-acetyl-maltose.

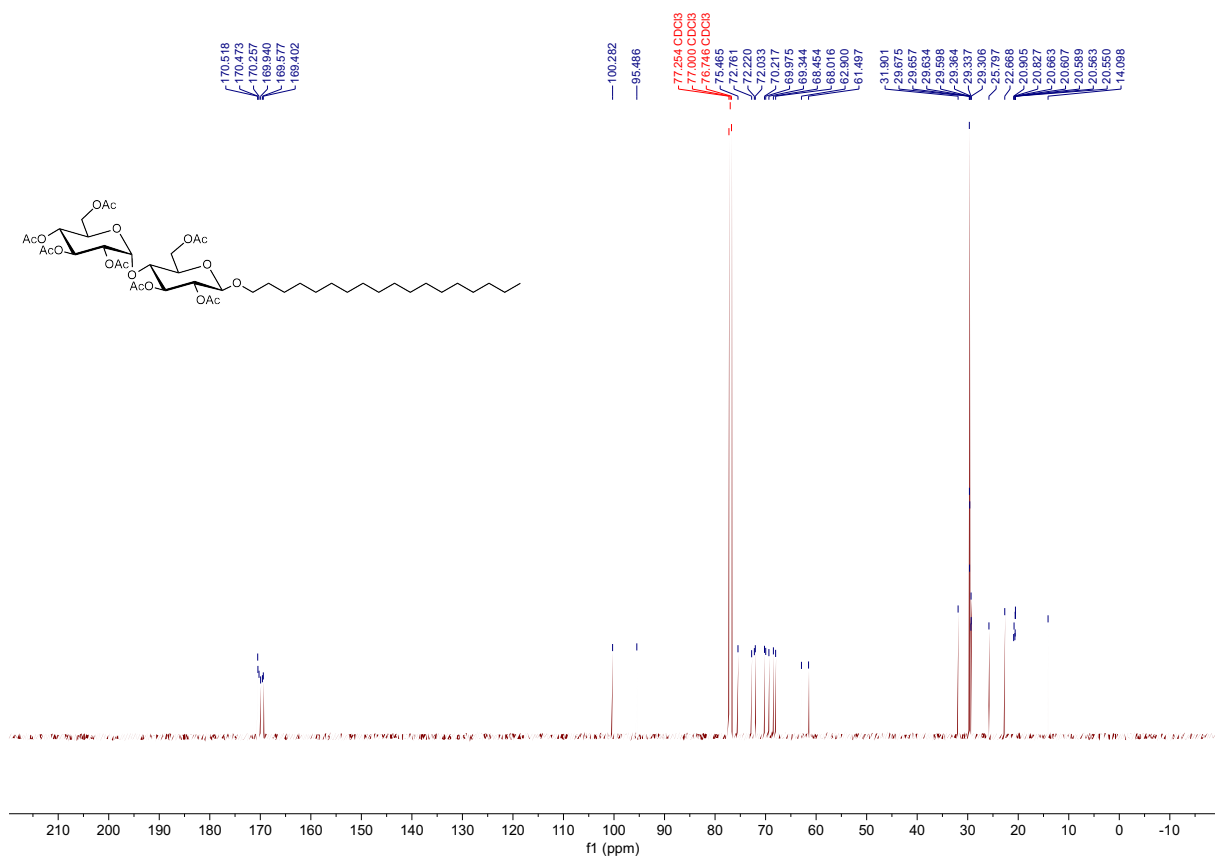


Fig. S32. ¹³C NMR spectrum of *O*-(octadecyl)-hepta-acetyl-maltose.

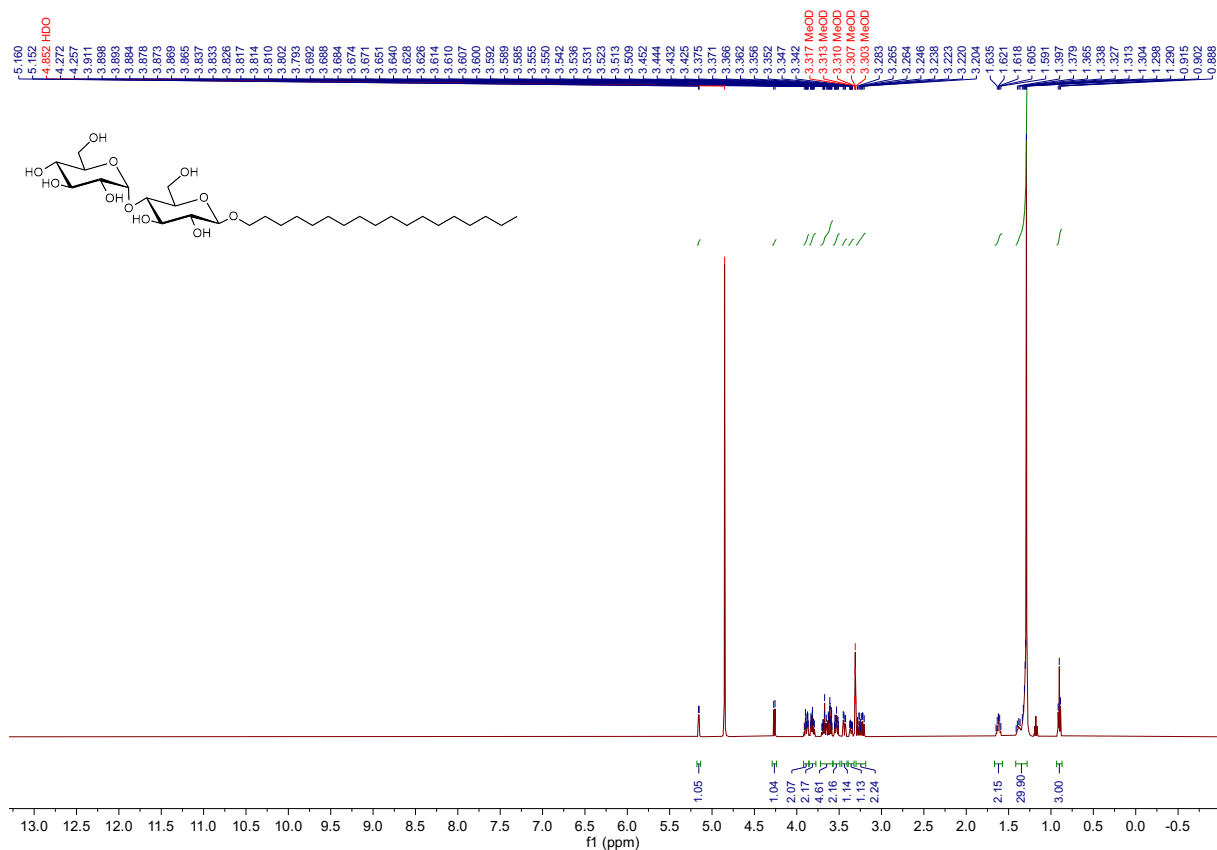


Fig. S33. ^1H NMR spectrum of (9-octadecynyl)- β -D-maltopyranoside.

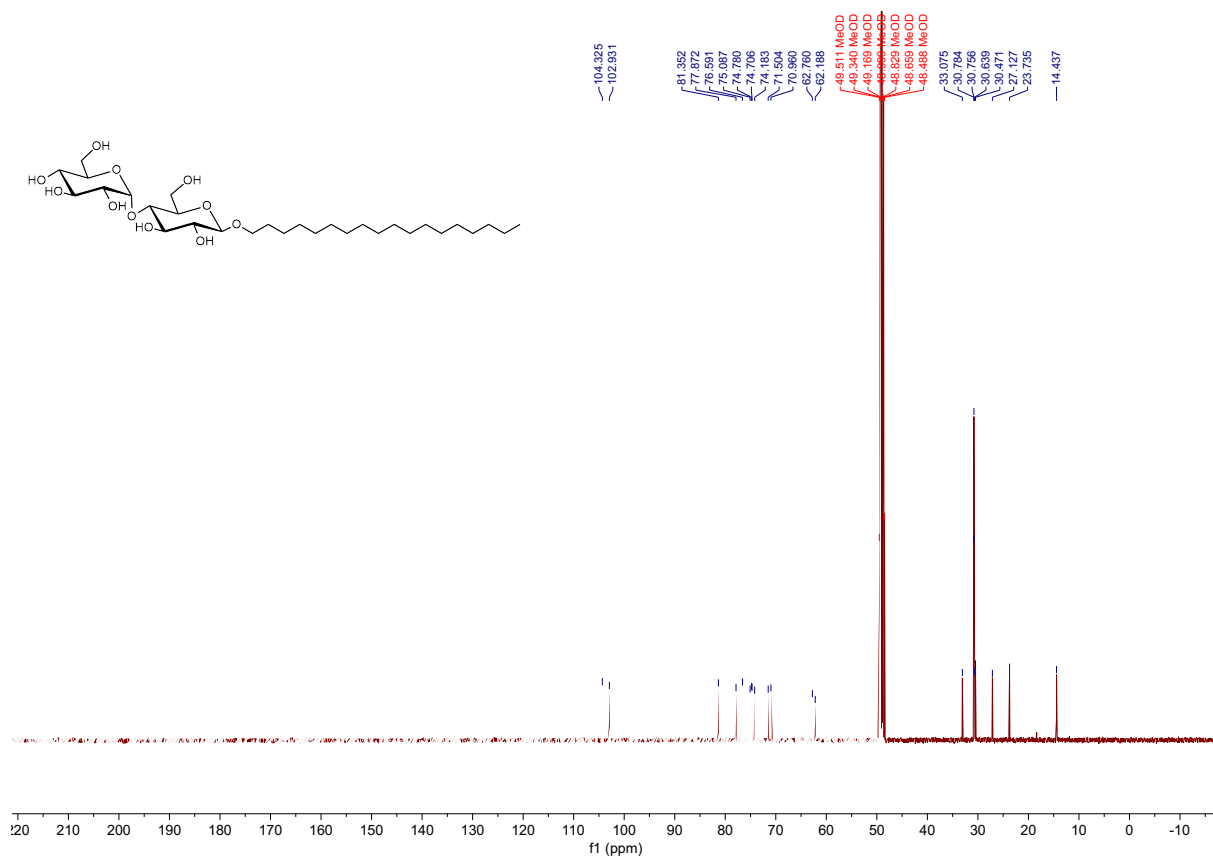


Fig. S34. ^{13}C NMR spectrum of (9-octadecynyl)- β -D-maltopyranoside.

3 Methods

Pyrene fluorescence assays were performed on a Probe Drum spectrophotometer (Probaton Labs Sweden AB). A solution of pyrene-1-aldehyde in Milli-Q water (100 nM, 1 mL) was added to a cuvette and incubated at 25 °C in a Probe Drum spectrophotometer (Probaton Labs Sweden AB). An aliquot of surfactant in Milli-Q water (1.005 mM, 5 μ L) was loaded to the sample cell followed by mixing under intermittent stirring for 60s. After equilibration for another 300s, the micelle formation was monitored by fluorescence ($\lambda_{\text{ex}} = 377$ nm, $\lambda_{\text{em}} = 350 - 650$ nm) in which two averages were recorded for the emission spectra. The addition-cycle was repeated until a total volume of 100 μ L has been added to the sample cell.

Differential scanning calorimetry was performed on a MicroCal VP-DSC instrument. An aliquot of surfactant in Milli-Q water (1.005 mM, 5 μ L) was loaded in Tzero pans (TA Instruments) and sealed. Signal was acquired between 5 – 95 °C at a scan rate of 30 °C/h with water as reference.

Dynamic light scattering (DLS) and static light scattering (SLS) measurements were performed using a 3D LS Spectrometer (LS Instruments) equipped with a goniometric optical setup and a 660 nm Cobolt (100 mW) light source. The instrument implements a modulated 3D cross-correlation scheme to suppress multiple scattering contributions. DLS data was acquired at a fixed angle of 110° (i.e., $q = 2.07 \times 10^{-3} \text{ \AA}^{-1}$). SLS data was collected within an angular range between 25° and 140°, resulting in a q -range of $6.55 \times 10^{-4} \text{ \AA}^{-1} \leq q \leq 2.28 \times 10^{-3} \text{ \AA}^{-1}$. The DLS intensity was processed by LS instrument correlators and the resulting intensity auto-correlation function ($g^2(q, t) - 1$) vs. lag time (t) was exported for analysis. The SLS data was converted to the excess Rayleigh ratio ($\Delta R(q)$) using toluene as reference solvent using the equation:

$$\Delta R(q) = \frac{I(q)_{\text{sample}}}{I(q)_{\text{toluene}}} \left(\frac{n_{D_2O}}{n_{\text{toluene}}} \right)^2 R_{\text{toluene}}$$

where $I(q)_{\text{sample}}$ and $I(q)_{\text{toluene}}$ are the measured intensities of the sample and the reference respectively, n_{D_2O} is the refractive index of D₂O and n_{toluene} is that of our reference, and R_{toluene} is the Rayleigh excess of the reference as determined with our setup ($0.8456 \times 10^{-5} \text{ cm}^{-1}$). Surfactants were characterised at a concentration of 1 mM in D₂O in SLS mode and DLS of β -C₁₈₋₉₂Mal in Milli-Q was measured at 0.1, 0.3, 0.5, 1, 2, 4, 6, 8, and 10 mM. The samples were loaded in 10-mm quartz tubes and placed into a temperature-controlled, index-matching vat at 25 °C.

Small-angle neutron scattering (SANS) experiments were performed on Sans2d (ISIS Pulsed Neutron Source, UK) using 5 m and 12 m sample-to-detector distances for the front and rear detector respectively.¹⁰ Using wavelengths between 1.75 and 12.5 \AA , the detectors yielded a combined q -range between 0.00156 and 0.5 \AA^{-1} . Samples were loaded in 2 mm path length, 1 cm width, quartz Hellma cells and placed in a temperature-controlled sample changer at a temperature of 25 °C. Data reduction was performed using Mantid with the standard procedures of the beamline., accounting for sample transmission, detector efficiency, and the scattering from an empty cell. The scattering of D₂O was subtracted as a background contribution accounting for the incoherent scattering from each sample. The data was absolutely scaled using the scattering from a standard sample (a solid blend of protiated and perdeuterated polystyrene) in accordance with established procedures. The resulting data present the absolute scattered intensities, $I(q)$ in cm^{-1} , versus momentum transfer, q in \AA^{-1} . Mathematical models were smeared accounting for the instrument resolution.

For MD Simulations, each surfactant molecule was initially constructed using the Avogadro software.¹¹ Then, the molecules were parametrised into the GROMOS 54A7 forcefield using the Automated Topology Builder and Repository Server.¹² The structures and corresponding files for Molecular Dynamics simulations are accessible through the following MolIDs: 1260813 for α -C_{18-9Z}Mal, 1260815 for β -C_{18-9Z}Mal, 1260816 for β -C_{18-9E}Mal, and 1260818 for β -C_{18-9Y}Mal. The topology files were then modified to ensure a common nomenclature across all the four molecules.

Four hundred units of each surfactant were then added to a cubic box of 17 nm side filled with SPC water molecules. The neutral systems were subjected to a steepest descent energy minimisation to remove atomic overlaps and clashes, followed by 1 ns NVT equilibration. The production trajectories were carried out at 1 bar and 298 K using the isotropic Parrinello-Rahman barostat and a Nose-Hoover thermostat.^{13, 14} The LINCS algorithm was employed to constrain bond lengths,¹⁵ thus eliminating bond vibrations and preventing system drift. The reaction-field method utilizing periodic boundary conditions was used to handle long-range electrostatics with a 1.0 nm cutoff in direct space.¹⁶ Van der Waals interactions were computed using a spherical cut-off of 1.0 nm. Production trajectories of 1.3 μ s with a time step of 2 fs for the integration of the motion equations were performed. Energies and positions of atoms were stored every 1000 (2 ps) steps. All MD simulations were performed with the GROMACS 2022.1 software package.¹⁷

Linear and oscillatory rheological measurements were carried out on Anton Paar MCR 301 at 25 °C using a cone-plate geometry with cone diameter of 25 mm, cone angle of 1°, and a gap of 0.048 mm. The flow curves were recorded in a shear rate range between 0.01 and 100 s⁻¹ with 7 measurements per decade. The linear viscoelastic region (LVER) was determined, and subsequent oscillatory measurements were conducted at a constant strain of 10% over the angular frequency range of 0.001–100 rad/s.

4 Data analysis

The DLS intensity autocorrelation functions were fitted using a second-order cumulant function:¹⁸

$$g_2(q, t) - 1 = B + \beta \left\{ \exp(-\Gamma_1 t) \left[1 + \frac{1}{2} \mu_2 t^2 \right] \right\}^2$$

where B represent baseline contributions, β is the spatial coherence factor, Γ_1 is the relaxation rate of the first cumulant, and μ_2 is the second cumulant that accounts for deviations from the single exponential behavior (e.g., polydispersity). The effective particle diffusion (D) was determined from the decay rate using the equation:

$$D = \frac{q^2}{\Gamma_1}$$

It should be noted that the fitting approach only accounts for the first relaxation mode (e.g., particle diffusion, network breathing).^{18, 19} Thus, slow relaxation modes (e.g., collective interactions) are not considered here.

Combined data from SANS and SLS measurements were analysed in SasView 5.0.5 using a model-based approach.²⁰ The Flexible Cylinder model was selected as the most appropriate considering the features of the scattering curves and previous investigations of similar systems.²¹ The scattering length density (SLD) of the micelle was calculated from the chemical composition of the protiated tail of the surfactant (i.e., $-0.39 \times 10^{-6} \text{ \AA}^{-2}$) and held constant. The

SLD of D₂O was fixed to $6.37 \times 10^{-6} \text{ \AA}^{-2}$. As the density-pair correlation considered by the model only accounts for the difference between the SLDs of the micelle and the solvent (i.e., $\text{SLD}_p - \text{SLD}_s$, where p and s stand for particle and solvent), discrepancies due to e.g., micelle hydration are only expected to cause subtle differences in the volume fraction of particles. That is, no variations in the structural parameters of the scatterers are foreseen. It should be noted that the size of the largest structural feature that can be resolved with the experimental setup used here is ca. 10000 \AA ($q_{\min} = 6.55 \times 10^{-4} \text{ \AA}^{-1}$). Larger values from that are estimated from the modelling of the data. The polydispersity in the radius of the micelle cross-section was fixed to 0.15 (Schulz distribution, number of points = 80, number of Sigmas = 8).²² Further details on the analysis protocols can be found in previous publications.^{23, 24} Fitting optimisation was performed using the Levenberg-Marquardt algorithm implemented in SasView 5.0.3. The tolerance was fixed to 1.5×10^{-8} and the reported uncertainties are within the 95% confidence level ($p = 0.05$).

Analyses of MD simulations data were performed on the final 100 ns of the simulation trajectories to ensure that the systems were well-equilibrated and to capture the relevant dynamic behavior of the surfactant molecules. Snapshots from the MD trajectories were generated using VMD providing a visual inspection of the molecular conformations and interactions.²⁵ The analysis of the simulations was carried out using the GROMACS *hbond* tool as well as specific code written in Python mainly based on the MDAnalysis,²⁶ Numpy and Matplotlib libraries.^{27, 28}

Oscillatory rheology data were analysed using the Maxwell model,²⁴ yielding the characteristic relaxation time (τ) and the plateau of the elastic modulus at high frequencies (G'_0). Data were adjusted using the Curve Fitting module implemented in IgorPro 8.04 and the least square algorithm.

5 Supplementary results

5.1 Solubility of glucoside- and maltoside-based surfactants

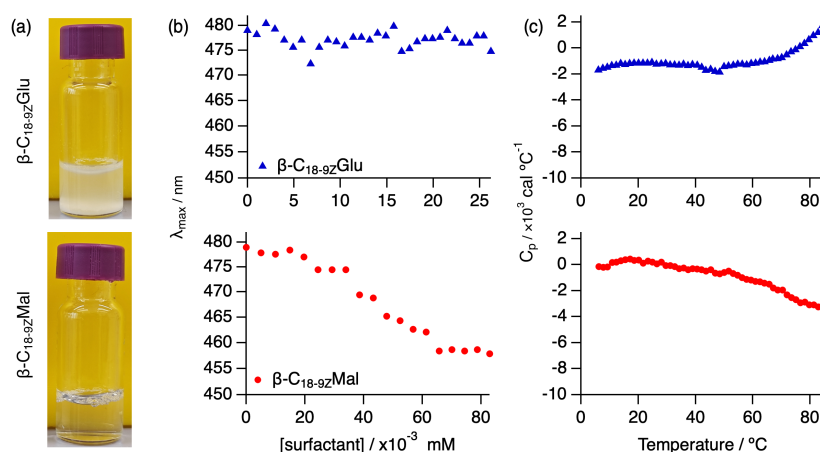


Fig. S35 Comparative behaviour of $\beta\text{-C}_{18-9Z}\text{Glu}$ and $\beta\text{-C}_{18-9Z}\text{Mal}$ in aqueous solution: (a) Images showing samples at room temperature with 25 mM surfactant concentration, (b) spectroscopic investigation of the CMC of the surfactants, and (c) DSC characterisation of the solubilisation temperature of the surfactants.

5.2 Determination of the solubilisation temperature

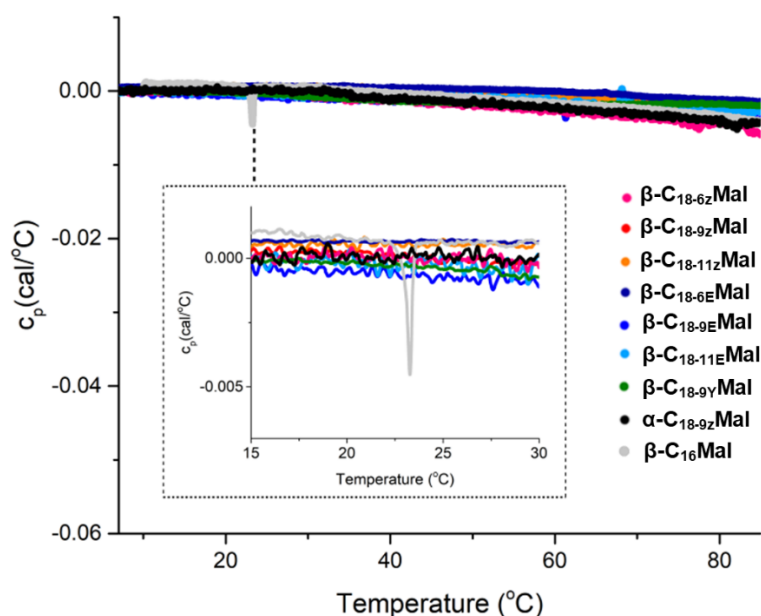


Fig. S36. c_p of sugar-based surfactants in H_2O determined by DSC. The signal from 1 mM β - C_{16} Mal in water was used as a control to confirm the response of the system.²⁹

5.3 Critical micelle concentration determination

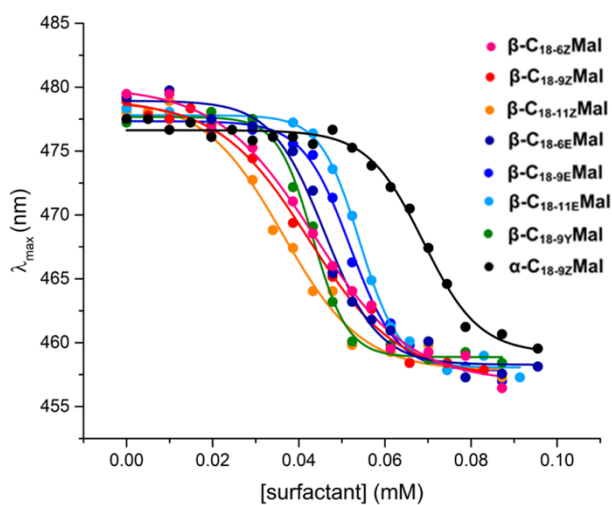


Fig. S37. Evolution of the fluorescence emission maximum of 1-pyrenecarboxylaldehyde upon titration with the different surfactants as indicated in the legend of the graph. The onset of the early transition (lower surfactant concentration) was used to determine the critical micelle concentration.

5.4 DLS correlation curves

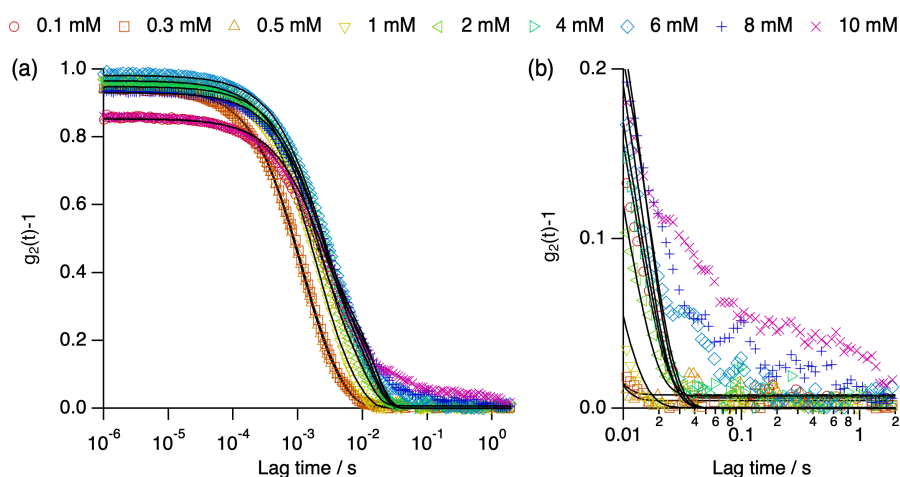


Fig. S38. (a) Intensity autocorrelation function of β -C_{18-9Z}Mal at different concentrations, as indicated in the graph legend, in Mili-Q water. Models are presented as black solid lines. (b) presents the signals obtained at long lag times (> 0.01 s).

5.5 Results from SANS/SLS data analysis

Table S1. Results from the model-based analysis of SANS data of the micelles from the different surfactants at a concentration of 1 mM: ϕ_p – volume fraction of scatterers, r – radius cross-section, l_p – persistence (statistical) length, L – contour length.

Surfactant	$\phi_p / \times 10^{-4}$	$r / \text{\AA}$	$l_p / \text{\AA}$	$L / \text{\AA}$
α -C _{18-9Z} Mal	3.8 ± 0.2	18.9 ± 0.6	252 ± 48	4750 ± 760
β -C _{18-9Z} Mal	2.6 ± 0.3	21.5 ± 0.5	123 ± 12	16200 ± 300
β -C _{18-9E} Mal	3.9 ± 0.2	21.9 ± 0.7	291 ± 26	28600 ± 700
β -C _{18-9Y} Mal	3.2 ± 0.2	19.8 ± 0.4	134 ± 17	9360 ± 110
β -C _{18-6Z} Mal	2.9 ± 0.1	20.8 ± 0.4	220 ± 11	16200 ± 600
β -C _{18-11Z} Mal	3.4 ± 0.2	22.0 ± 0.3	270 ± 20	21000 ± 600
β -C _{18-6E} Mal	4.1 ± 0.1	22.1 ± 0.5	316 ± 21	22400 ± 700
β -C _{18-11Z} Mal	3.2 ± 0.1	22.3 ± 0.5	370 ± 12	23300 ± 700

5.6 MD simulation snapshots

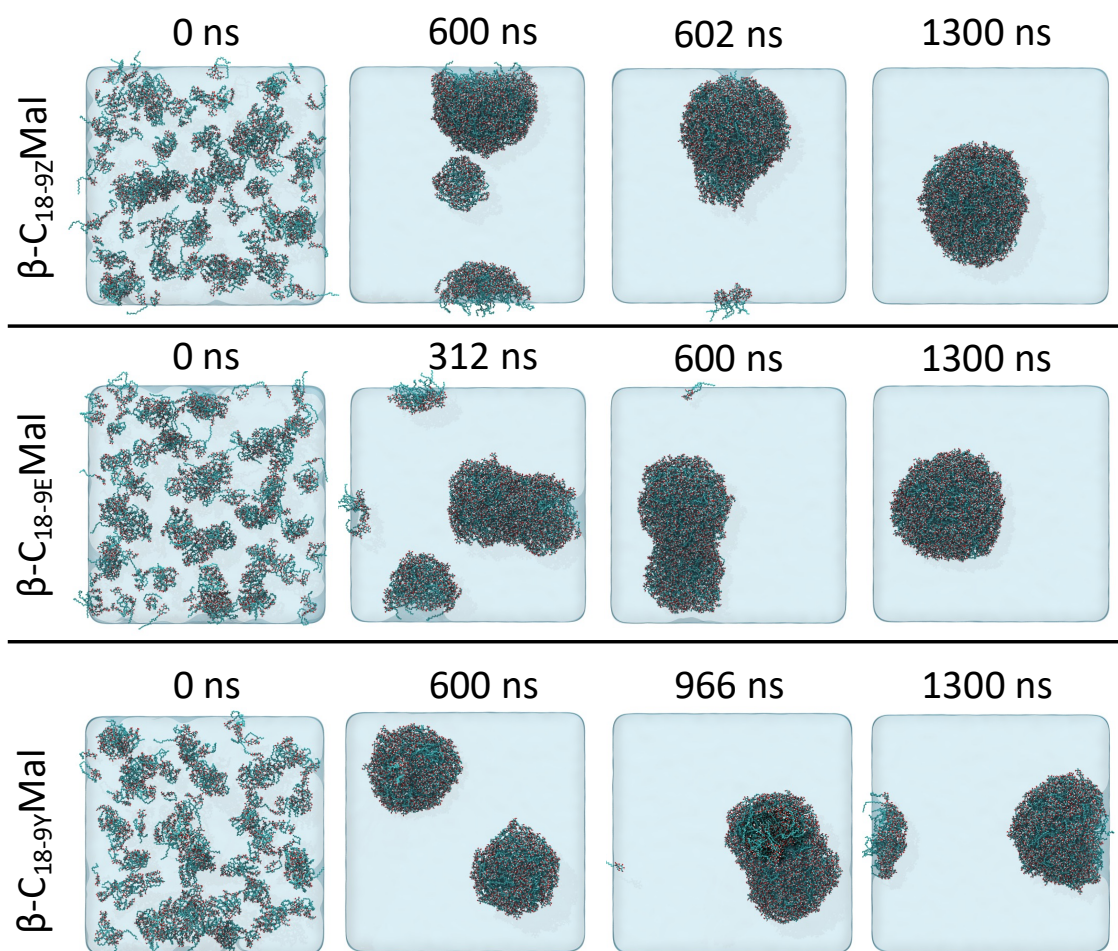


Fig. S39. (a) Representative snapshots of the MD simulation trajectory of different surfactants conducted at 1 bar and 298.15 K.

5.7 Linear rheology results

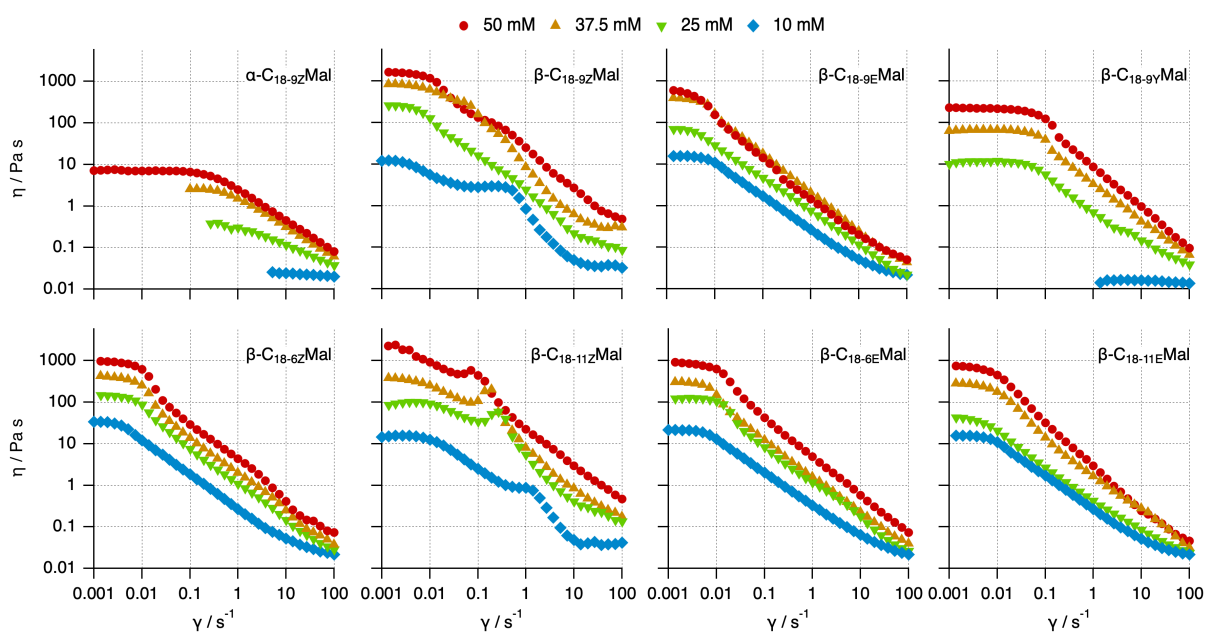


Fig. S40. Linear viscosity ramps as a function of the shear rate for the surfactants at different concentrations in aqueous solution as indicated in the graph legend.

5.8 Oscillatory rheology results

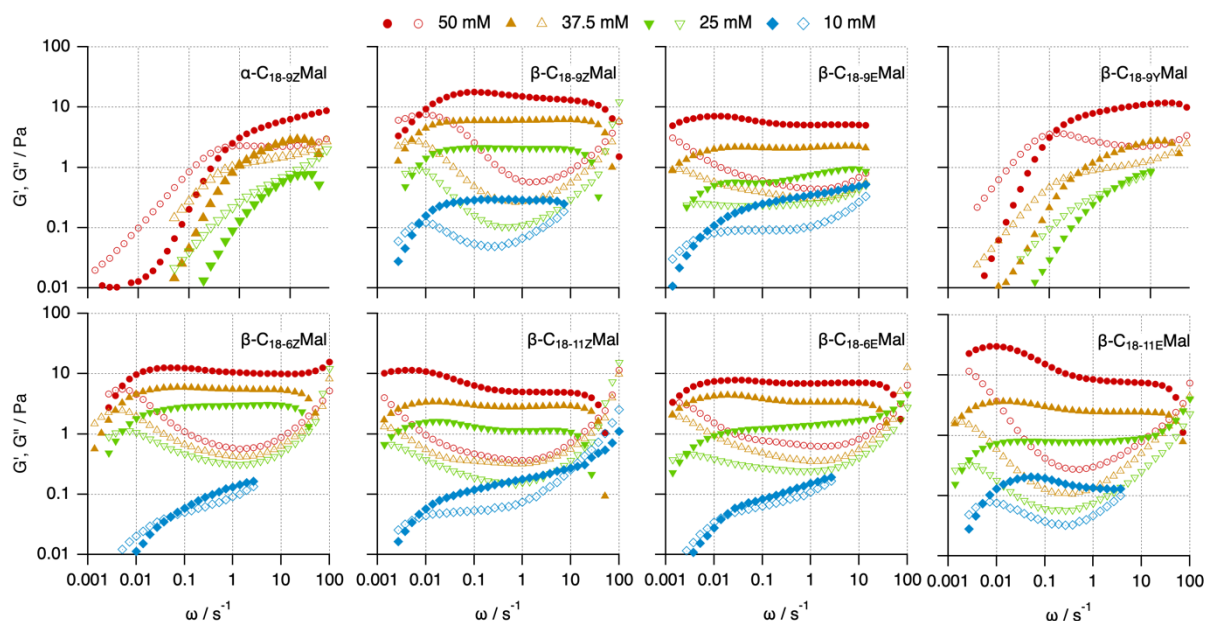


Fig. S41. Oscillatory shear frequency-sweep results (strain of 10%) for the surfactants at different concentrations in aqueous solution as indicated in the graph legend. Data are represented as the elastic (G' , open symbols) and viscous (G'' , filled symbols) moduli as a function of frequency. Surfactant concentrations are indicated on the graph legend.

5.9 Cole-Cole plots

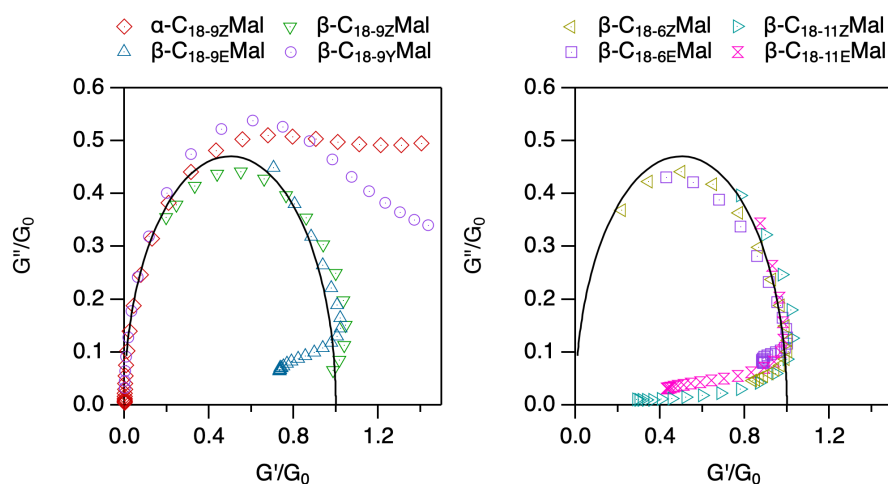


Fig. S42. Normalised Cole-Cole plots obtained from the shear frequency-sweep results (strain of 10%) for 50 mM of surfactants as indicated in the legend of the graphs.

6 Supporting references

1. P. E. Duffy, S. M. Quinn, H. M. Roche and P. Evans, *Tetrahedron*, 2006, **62**, 4838-4843.
2. S. Orgies, R. Rieger, K. Rode, K. Koszinowski, J. Kind, C. M. Thiele, J. Rehbein and A. Breder, *ACS Catalysis*, 2017, **7**, 7578-7586.

3. M. Overs, M. Fix, S. Jacobi, L. F. Chi, M. Sieber, H.-J. Schäfer, H. Fuchs and H.-J. Galla, *Langmuir*, 1999, **16**, 1141-1148.
4. J. Yue and S. S. Narine, *Chem. Phys. Lipids*, 2008, **152**, 1-8.
5. C. Koga, M. Kohri, T. Taniguchi and K. Kishikawa, *J. Phys. Chem. B*, 2019, **123**, 4324-4332.
6. S. Narasimhan, K. G. Prasad and S. Madhavan, *Tetrahedron Lett.*, 1995, **36**, 1141-1144.
7. T. Zheng, R. S. Narayan, J. M. Schomaker and B. Borhan, *J. Am. Chem. Soc.*, 2005, **127**, 6946-6947.
8. A. Sytniczuk, M. Dabrowski, L. Banach, M. Urban, S. Czarnocka-Sniadala, M. Milewski, A. Kajetanowicz and K. Grela, *J. Am. Chem. Soc.*, 2018, **140**, 8895-8901.
9. S.-S. Kim and Y. P. Hong, *Bull. Korean Chem. Soc.*, 2011, **32**, 3120-3122.
10. R. K. Heenan, S. E. Rogers, D. Turner, A. E. Terry, J. Treadgold and S. M. King, *Neutron News*, 2011, **22**, 19-21.
11. M. D. Hanwell, D. E. Curtis, D. C. Lonie, T. Vandermeersch, E. Zurek and G. R. Hutchison, *J Cheminform*, 2012, **4**, 17.
12. N. Schmid, A. P. Eichenberger, A. Choutko, S. Riniker, M. Winger, A. E. Mark and W. F. van Gunsteren, *Eur. Biophys. J.*, 2011, **40**, 843-856.
13. M. Parrinello and A. Rahman, *J. Appl. Phys.*, 1981, **52**, 7182-7190.
14. D. J. Evans and B. L. Holian, *J. Chem. Phys.*, 1985, **83**, 4069-4074.
15. B. Hess, H. Bekker, H. J. C. Berendsen and J. G. E. M. Fraaije, *J. Comput. Chem.*, 1997, **18**, 1463-1472.
16. P. H. Hünenberger and W. F. van Gunsteren, *J. Chem. Phys.*, 1998, **108**, 6117-6134.
17. M. J. Abraham, T. Murtola, R. Schulz, S. Páll, J. C. Smith, B. Hess and E. Lindahl, *SoftwareX*, 2015, **1-2**, 19-25.
18. A. Gulotta, M. Polimeni, S. Lenton, C. G. Starr, A. Stradner, E. Zaccarelli and P. Schurtenberger, *Mol. Pharm.*, 2024, **21**, 2250-2271.
19. A. Sanchez-Fernandez, J. Larsson, A. E. Leung, P. Holmqvist, O. Czakkel, T. Nylander, S. Ulvenlund and M. Wahlgren, *Langmuir*, 2022, **38**, 10075-10080.
20. M. Doucet, J. H. Cho, G. Alina, Z. Attala, J. Bakker, W. Bouwman, P. Butler, K. Campbell, T. Cooper-Benun, C. Durniak, L. Forster, M. Gonzales, R. Heenan, A. Jackson, S. King, P. Kienzle, J. Krzywon, T. Nielsen, L. O'Driscoll, W. Potrzebowski, S. Prescott, R. Ferraz Leal, P. Rozycko, T. Snow and A. Washington, SasView version 5.0.3, <https://zenodo.org/record/3930098>, (accessed 2020-08-24, DOI: 10.5281/ZENODO.3930098).
21. J. S. Pedersen and P. Schurtenberger, *Macromolecules*, 1996, **29**, 7602-7612.
22. M. Kotlarchyk, R. B. Stephens and J. S. Huang, *J. Phys. Chem.*, 2002, **92**, 1533-1538.
23. J. Larsson, A. Sanchez-Fernandez, N. Mahmoudi, L. C. Barnsley, M. Wahlgren, T. Nylander and S. Ulvenlund, *Langmuir*, 2019, **35**, 13904-13914.
24. J. Larsson, A. Sanchez-Fernandez, A. E. Leung, R. Schweins, B. Wu, T. Nylander, S. Ulvenlund and M. Wahlgren, *J. Colloid Interface Sci.*, 2021, **581**, 895-904.
25. W. Humphrey, A. Dalke and K. Schulten, *J Mol Graph*, 1996, **14**, 33-38, 27-38.

26. N. Michaud-Agrawal, E. J. Denning, T. B. Woolf and O. Beckstein, *J. Comput. Chem.*, 2011, **32**, 2319-2327.
27. J. D. Hunter, *Computing in Science & Engineering*, 2007, **9**, 90-95.
28. C. R. Harris, K. J. Millman, S. J. van der Walt, R. Gommers, P. Virtanen, D. Cournapeau, E. Wieser, J. Taylor, S. Berg, N. J. Smith, R. Kern, M. Picus, S. Hoyer, M. H. van Kerkwijk, M. Brett, A. Haldane, J. F. Del Rio, M. Wiebe, P. Peterson, P. Gerard-Marchant, K. Sheppard, T. Reddy, W. Weckesser, H. Abbasi, C. Gohlke and T. E. Oliphant, *Nature*, 2020, **585**, 357-362.
29. J. Larsson, A. E. Leung, C. Lang, B. Wu, M. Wahlgren, T. Nylander, S. Ulvenlund and A. Sanchez-Fernandez, *J. Colloid Interface Sci.*, 2021, **585**, 178-183.